CONVERGENCE OF A VARIANT OF THE ZIPPER ALGORITHM FOR CONFORMAL MAPPING[*]

DONALD E. MARSHALL[†] AND STEFFEN ROHDE[†]

Abstract. In the early 1980s an elementary algorithm for computing conformal maps was discovered by R. Kühnau and the first author. The algorithm is fast and accurate, but convergence was not known. Given points $z_0, \ldots, z_n$ in the plane, the algorithm computes an explicit conformal map of the unit disk onto a region bounded by a Jordan curve γ with $z_0, \ldots, z_n \in \gamma$. We prove convergence for Jordan regions in the sense of uniformly close boundaries and give corresponding uniform estimates on the closed region and the closed disc for the mapping functions and their inverses. Improved estimates are obtained if the data points lie on a C^1 curve or a K-quasicircle. The algorithm was discovered as an approximate method for conformal welding; however, it can also be viewed as a discretization of the Loewner differential equation.

Key words. numerical conformal mapping, zipper algorithm, hyperbolic geodesics

AMS subject classifications. Primary, 30C30; Secondary, 65E05

DOI. 10.1137/060659119

Introduction. Conformal maps have applications to problems in physics, engineering, and mathematics, but how do you find a conformal map, say, of the upper-half plane $\mathbb{H}$ to a complicated region? Rather few maps can be given explicitly by hand, so that a computer must be used to find the map approximately. One reasonable way to describe a region numerically is to give a large number of points on the boundary (see Figure 1). One way to say that a computed map defined on $\mathbb{H}$ is "close" to a map to the region is to require that the boundary of the image be uniformly close to the polygonal curve through the data points. Indeed, the only information we may have about the boundary of a region is this collection of data points.

In the early 1980s an elementary algorithm was discovered independently by Kühnau [K] and the first author. The algorithm is fast and accurate, but convergence was not known. The purpose of this paper is to prove convergence in the sense of uniformly close boundaries and discuss related numerical issues. In many applications both the conformal map and its inverse are required. One important aspect of the algorithm that sets it apart from others is that this algorithm finds both maps simultaneously.

The algorithm can be viewed as an approximate solution to a conformal welding problem or as a discretization of the Loewner differential equation. The approximation to the conformal map is obtained as a composition of conformal maps onto slit half planes. Osculation methods also approximate a conformal map by repeated composition of simple maps. See Henrici [H] for a discussion of osculation methods and uniform convergence on compact sets. The algorithms of the present article follow the boundary of a given region much more closely than, for instance, the Koebe algorithm and give uniform convergence on all of $\mathbb{H}$ rather than just on compact subsets. Uniform convergence on the closure of the region is particularly important in applications

---

[†]Department of Mathematics, University of Washington, Seattle, WA 98195-4350 (marshall@math.washington.edu, rohde@math.washington.edu).
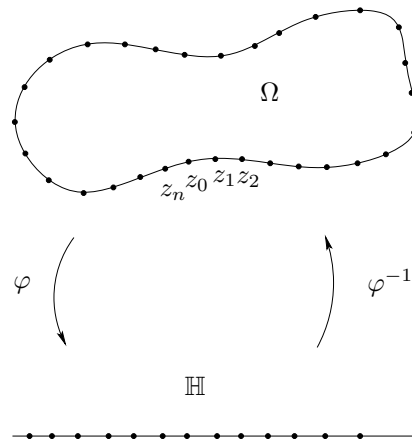
that involve boundary values of functions defined on the region. It is possible to use the techniques of this paper to prove that a version of the algorithm is an osculation method for smooth curves, and therefore by the results in [H] repeated applications converge, in the weaker sense, uniformly on compact subsets. However, prior to this article, even a proof that these methods satisfied the osculation family conditions was not known.

Depending on the type of slit (hyperbolic geodesic, straight line segment, or circular arc) we actually obtain different versions of this algorithm. These are described in section 1. We then focus our attention on the "geodesic algorithm" and study its behavior in different situations. The easiest case is discussed in section 2: If the data points $z_0, z_1, \ldots$ are the consecutive contact points of a chain of disjoint discs (see Figures 7 and 8 below), then a simple but very useful reinterpretation of the algorithm, together with the hyperbolic convexity of discs in simply connected domains (Jørgensen's theorem), implies that the curve produced by the algorithm is confined to the chain of discs (Theorem 2.2). One consequence is that for any bounded simply connected domain Ω, the geodesic algorithm can be used to compute a conformal map to a Jordan region Ω_c ("c" is for "computed") so that the Hausdorff distance between $\partial\Omega$ and $\partial\Omega_c$ is as small as desired (Theorem 2.4).

In section 3, we describe an extension of the ideas of section 2 that applies to a variety of domains such as smooth domains or quasiconformal discs with small constants, with better estimates. For instance, if $\partial\Omega$ is a C^1 curve, then the geodesic algorithm can be used to compute a conformal map to a Jordan region Ω_c with $\partial\Omega_c \in C^1$ so that the boundaries are uniformly close and so that the unit tangent vectors are uniformly close (Theorem 3.10). The heart of the convergence proof in these cases comprises the technical "self-improvement" in Lemmas 3.5 and 3.6. In fact, this approach constituted our first convergence proof.

In sections 4 and 5, we show how estimates on the distance between boundaries of Jordan regions give estimates for the uniform distance between the corresponding conformal maps to $\mathbb{D}$, and we apply these estimates to obtain bounds for the convergence of the conformal maps produced by the algorithm. We summarize some of our results as follows: If $\partial\Omega$ is contained in a chain of discs of radius $\leq \epsilon$ with the data points being the contact points of the discs, or if $\partial\Omega$ is a K-quasicircle with K close to one and the data points are consecutive points on $\partial\Omega$ of distance comparable to ϵ,

then the Hausdorff distance between $\partial\Omega$ and the boundary of the domain computed by the geodesic algorithm, $\partial\Omega_c$, is at most ε. Moreover, the conformal maps φ, φ_c onto $\mathbb{D}$ satisfy

$$\sup_{\Omega \cap \Omega_c} |\varphi - \varphi_c| \le C\epsilon^p,$$

where any $p < 1/2$ works in the disc-chain case, and p is close to one if K is close to one. In the case of quasicircles, we also have

$$\sup_{\mathbb{D}} |\varphi^{-1} - \varphi_c^{-1}| \le C\epsilon^p$$

with p close to one. Better estimates are obtained for regions bounded by smoother Jordan curves.

Section 6 contains a brief discussion of numerical results. The appendix has a simple self-contained proof of Jørgensen's theorem.

In a forthcoming paper we plan to address the convergence of the slit and zipper variants of the algorithm. The basic conformal maps and their inverses used in the geodesic algorithm are given in terms of linear fractional transformations, squares, and square roots. The slit and zipper algorithms use elementary maps whose inverses cannot be written in terms of elementary maps. In that paper we will discuss how to divide the plane into four regions so that Newton's method applied to variants of the inverses will converge quadratically in each region. Newton's method converges so rapidly that it virtually provides a formula for the inverses.

1. Conformal mapping algorithms. The geodesic algorithm. The most elementary version of the conformal mapping algorithm is based on the simple map $f_a : \mathbb{H} \setminus \gamma \longrightarrow \mathbb{H}$, where γ is an arc of a circle from 0 to $a \in \mathbb{H}$ which is orthogonal to $\mathbb{R}$ at 0.

This map can be realized by a composition of a linear fractional transformation, the square, and the square root map, as illustrated in Figure 2. The orthogonal circle
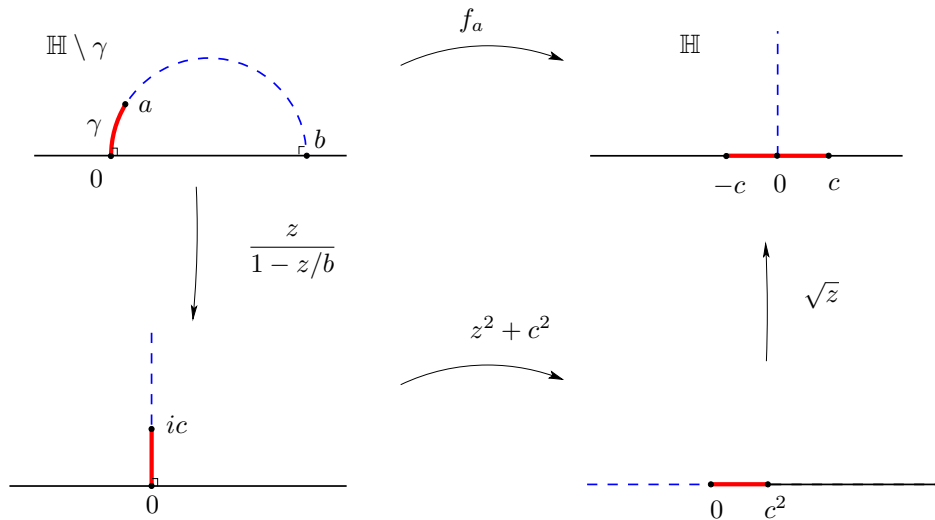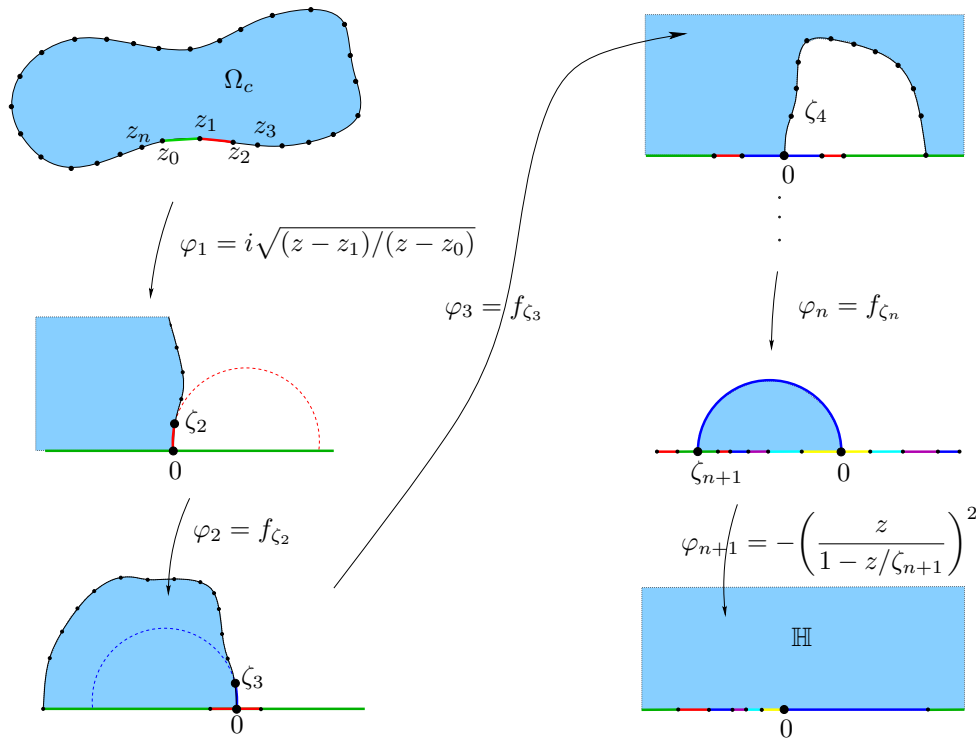

Fig. 2. *The basic map f_a.*

FIG. 3. *The geodesic algorithm.*

also meets $\mathbb{R}$ orthogonally at a point $b = |a|^2/\operatorname{Re} a$ and is illustrated by a dashed curve in Figure 2. In Figure 2, $c = |a|^2/\operatorname{Im} a$. Observe that the arc γ is opened to two adjacent intervals at 0 with a, the tip of γ, mapped to 0. The inverse f_a^{-1} can be easily found by composing the inverses of these elementary maps in the reverse order.

Now suppose that $z_0, z_1, \ldots, z_n$ are points in the plane. The basic maps f_a can be used to compute a conformal map of $\mathbb{H}$ onto a region Ω_c bounded by a Jordan curve which passes through the data points, as illustrated in Figure 3.

The complement in the extended plane of the line segment from z_0 to z_1 can be mapped onto $\mathbb{H}$ with the map

$$\varphi_1(z) = i\sqrt{\frac{z - z_1}{z - z_0}},$$

$\varphi_1(z_1) = 0$, and $\varphi_1(z_0) = \infty$. Set $\zeta_2 = \varphi_1(z_2)$ and $\varphi_2 = f_{\zeta_2}$. Repeating this process, define

$$\zeta_k = \varphi_{k-1} \circ \varphi_{k-2} \circ \cdots \circ \varphi_1(z_k)$$

and

$$\varphi_k = f_{\zeta_k}$$

for $k = 2, \ldots, n$. Finally, map a half disc to $\mathbb{H}$ by letting

$$\zeta_{n+1} = \varphi_n \circ \cdots \circ \varphi_1(z_0) \in \mathbb{R}$$

be the image of z_0, and set

$$\varphi_{n+1} = \pm \left(\frac{z}{1 - z/\zeta_{n+1}} \right)^2.$$

The $+$ sign is chosen in the definition of φ_{n+1} if the data points have a negative winding number (clockwise) around an interior point of $\partial\Omega$, and otherwise the $-$ sign is chosen. Set

$$\varphi = \varphi_{n+1} \circ \varphi_n \circ \cdots \circ \varphi_2 \circ \varphi_1$$

and

$$\varphi^{-1} = \varphi_1^{-1} \circ \varphi_2^{-1} \circ \cdots \circ \varphi_{n+1}^{-1}.$$

Then φ^{-1} is a conformal map of $\mathbb{H}$ onto a region Ω_c such that $z_j \in \partial\Omega_c$, $j = 0, \ldots, n$. The portion γ_j of $\partial\Omega_c$ between z_j and z_{j+1} is the image of the arc of a circle in the upper-half plane by the analytic map $\varphi_1^{-1} \circ \cdots \circ \varphi_j^{-1}$. In more picturesque language, after applying φ_1, we grab the ends of the displayed horizontal line segment and pull, splitting apart or unzipping the curve at 0. The remaining data points move down until they hit 0, and then each splits into two points, one on each side of 0, moving further apart as we continue to pull.

As an aside, we make a few comments. As mentioned, $\partial\Omega_c$ is piecewise analytic. A curve is called C^1 if the arc length parameterization has a continuous first derivative. In other words, the direction of the unit tangent vector is continuous. It is easy to see that $\partial\Omega_c$ is also C^1 since the inverse of the basic map f_a in Figure 2 doubles angles at 0 and halves angles at $\pm c$. In fact, it is also $C^{\frac{3}{2}}$ (see Proposition 3.12). If the data points $\{z_j\}$ lie on the boundary of a given region $\partial\Omega$, the analyticity of $\partial\Omega_c$ also allows us in many situations (see Proposition 2.5 and Corollary 3.9) to extend φ_c analytically across $\partial\Omega_c$ so that the extended map is a conformal map of Ω onto a region with boundary very close to $\partial\mathbb{D}$. Note also that φ is a conformal map of the complement of Ω_c, $\mathbb{C}^* \setminus \overline{\Omega_c}$, onto the lower-half plane, $\mathbb{C} \setminus \overline{\mathbb{H}}$, where $\mathbb{C}^*$ denotes the extended plane. Simply follow the unshaded region in $\mathbb{H}$ in Figure 3. Finally, we remark that it is easier to use geodesic arcs in the right-half plane instead of in the upper-half plane when coding the algorithm because of the usual convention that $-\frac{\pi}{2} < \arg \sqrt{z} \le \frac{\pi}{2}$.

The slit algorithm. Given a region Ω, we can select boundary points $z_0, \ldots, z_n$ on $\partial\Omega$ and apply the geodesic algorithm. We can view the circular arcs γ for the basic maps f_a as approximating the image of the boundary of Ω between 0 and a with a circular arc at each stage. We can improve the approximation by using straight lines instead of orthogonal arcs. So in the slit algorithm we replace the inverse of the maps f_a by conformal maps $g_a : \mathbb{H} \longrightarrow \mathbb{H} \setminus L$, where L is a line segment from 0 to a. Explicitly

$$g_a(z) = C(z - p)^p (z + 1 - p)^{1-p},$$

where $p = \arg a / \pi$ and $C = |a| / p^p (1 - p)^{1-p}$.

One way to see that g_a is a conformal map is to note that as x traces the real line from $-\infty$ to $+\infty$, $g_a(x)$ traces the boundary of $\mathbb{H} \setminus L$ and $g_a(z) \sim Cz$ for large z, and then apply the argument principle. Another method would be to construct $\operatorname{Re} \log g_a$ using harmonic measure, as in the first two pages of [GM]. As in the basic maps of the
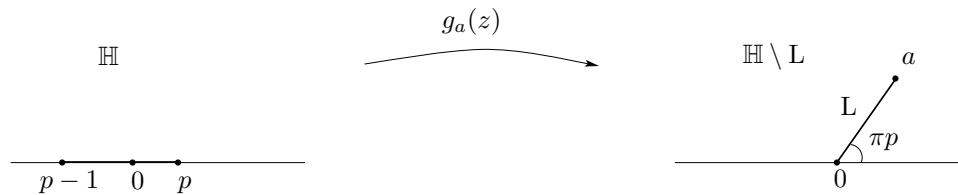
$$g_a(z)$$

$\mathbb{H}$

$\mathbb{H} \setminus \mathrm{L}$ a

L

πp

$p-1 \quad 0 \quad p$

0

FIG. 4. *The slit maps.*

geodesic algorithm, the line segment from 0 to a is opened to two adjacent intervals on $\mathbb{R}$ by $f_a = g_a^{-1}$ with $f_a(a) = 0$ and $f_a(\infty) = \infty$. The map f_a cannot be written in terms of elementary functions, but an effective and rapid numerical inverse will be described in a subsequent paper.

We note that, as in the geodesic algorithm, the boundary of the region Ω_c computed with the slit algorithm will be piecewise analytic. However, it will not be C^1. Indeed, if g_a is the map illustrated by Figure 4, and if g_b is another such map, then $g_b \circ g_a$ forms a curve with angles $2\pi p$ and $2\pi(1 - p)$ on either side of the curve at $b = g_b(0)$. Since analytic maps preserve angles, the boundary of the computed region consists of analytic arcs with endpoints at the data points, and angles determined by the basic maps. This will allow us to accurately compute conformal maps to regions with (a finite number of) "corners" or "bends."

The zipper algorithm. We can further improve the approximation by replacing the linear slits with arcs of (nonorthogonal) circles. In this version we assume there is an even number of boundary points, $z_0, z_1, \ldots, z_{2n+1}$. The first map is replaced by

$$\varphi_1(z) = \sqrt{\frac{(z - z_2)(z_1 - z_0)}{(z - z_0)(z_1 - z_2)}},$$

which maps the complement in the extended plane of the circular arc through z_0, z_1, z_2 onto $\mathbb{H}$. At each subsequent stage, instead of pulling down one point ζ_k, we can find a unique circular arc through 0 and the (images of) the next two data points ζ_{2k-1} and ζ_{2k}. By a linear fractional transformation ℓ_a which preserves $\mathbb{H}$, this arc is mapped to a line segment (assuming the arc is not tangent to $\mathbb{R}$ at 0). See Figure 5.

The complement of this segment in $\mathbb{H}$ can then be mapped to $\mathbb{H}$ as described in the slit algorithm, using g_d^{-1}, where $d = a/(1 - a/b)$. The composition $h_{a,c} = g_d^{-1} \circ \ell_a$ then maps the complement of the circular arc in $\mathbb{H}$ onto $\mathbb{H}$. Thus at each stage we are giving a "quadratic approximation" instead of a linear approximation to the (image of) the boundary. The last map φ_{n+1} is a conformal map of the intersection of a disc with $\mathbb{H}$ where the boundary circular arc passes through 0, the image of z_{2n+1}, and the image of z_0 by the composition $\varphi_n \circ \cdots \circ \varphi_1$. See Figure 6.

If the zipper algorithm is used to approximate the boundary of a region with bends or angles at some boundary points, then better accuracy is obtained if the bends occur only at even numbered vertices $\{z_{2n}\}$, $n \neq 0$.

Conformal welding. The discovery of the slit algorithm by the first author came from considering conformal weldings. (The simpler geodesic algorithm was discovered later.) A decreasing continuous function $h : [0, +\infty) \to (-\infty, 0]$ with $h(0) = 0$ is called a *conformal welding* if there is a conformal map f of $\mathbb{H}$ onto $\mathbb{C} \setminus \gamma$, where γ is a Jordan arc from 0 to ∞ such that $f(x) = f(h(x))$ for $x \in [0, +\infty)$. In other words, the map f pastes the negative and positive real half lines together according to the
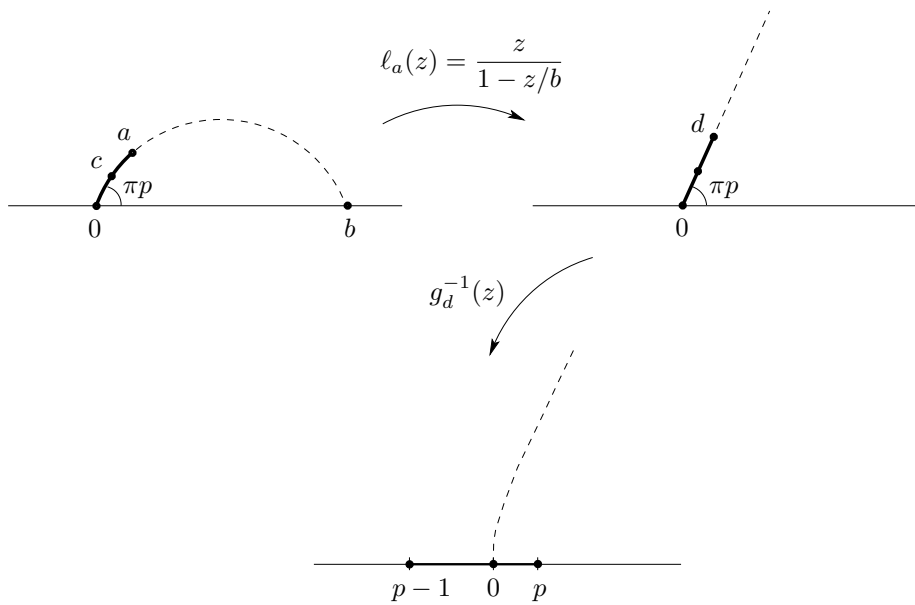
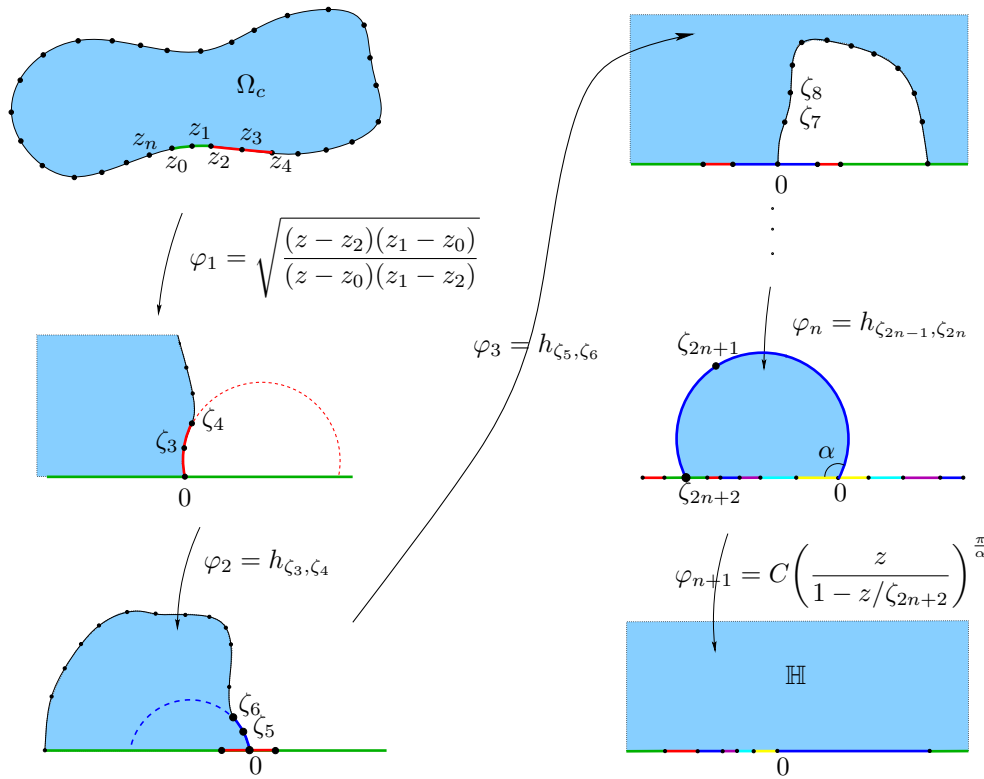FIG. 5. *The circular slit maps.*

FIG. 6. *The zipper algorithm.*

prescription h to form a curve. One way to approximate a conformal welding is to prescribe the map h at finitely many points and then construct a conformal mapping of $\mathbb{H}$ which identifies the associated intervals.

A related problem, which the first author considered in joint work with L. Carleson, is as follows: Given angles $\alpha_1, \alpha_2, \ldots, \alpha_n$ and $0 < x_1 < x_2 < \cdots < x_n$, find points $y_n < \cdots < y_1 < 0$ so that there is a Schwarz–Christoffel map f of $\mathbb{H}$ onto a region bounded by a polygonal arc tending to ∞ with angles $\alpha_j, 2\pi - \alpha_j$ at the jth vertex $f(x_j) = f(y_j)$. This map welds the intervals $[x_j, x_{j+1}]$ and $[y_{j+1}, y_j]$, $j = 1, \ldots, n$. Unfortunately, at the time the best Schwarz–Christoffel method was only fast enough to do this problem with polygonal curves with up to 20 bends.

The basic maps g_a can be used to compute the conformal maps of weldings. Indeed, suppose $y_1 < 0 < x_1$, let $a = x_1/(x_1 - y_1)$, and apply the map $g_a(z/(x_1 - y_1))$. This map identifies the intervals $[y_1, 0]$ and $[0, x_1]$ by mapping them to the two "sides" of a line segment $L \subset \mathbb{H}$. Composing maps of this form will give a conformal map $\varphi : \mathbb{H} \to \mathbb{C} \setminus \gamma$ such that $\varphi([x_j, x_{j+1}]) = \varphi([y_{j+1}, y_j])$. The final intervals are welded together using the map z^2. The numerical computation of these maps is easily fast enough to compose 10^5 basic maps, thereby giving an approximation to almost any conformal welding. Conversely, given a Jordan arc γ connecting 0 to ∞, the associated welding can be found approximately by using the slit algorithm to approximate the conformal map from $\mathbb{H}$ to the complement of γ.

From this point of view, the slit or the geodesic algorithms find the conformal welding of a curve (approximately). From the point of view of increasing the boundary via a small curve γ_j from z_j to z_{j+1}, the algorithms are discrete solutions of Loewner's differential equation.

The idea of closing up such a region using a map of the form φ_{n+1} was suggested by L. Carleson, for which we thank him.

2. Disc-chains. The geodesic algorithm can be applied to any sequence of data points $z_0, z_1, \ldots, z_n$, unless the points are out of order in the sense that a data point z_j belongs to the geodesic from z_{k-1} to z_k for some $k < j$. In this section we will give a simple condition on the data points $z_0, z_1, \ldots, z_n$ which is sufficient to guarantee that the curve computed by the geodesic algorithm is close to the polygon with vertices $\{z_j\}$.

DEFINITION 2.1. *A disc-chain $D_0, D_1, \ldots, D_n$ is a sequence of pairwise disjoint open discs such that ∂D_j is tangent to ∂D_{j+1} for $j = 0, \ldots, n-1$. A closed disc-chain is a disc-chain such that ∂D_n is tangent to ∂D_0.*

Any closed Jordan polygon P, for example, can be covered by (the closure of) a closed disc-chain with arbitrarily small radii and centers on P (see Figure 7). There are several ways to accomplish this, but one straightforward method is the following: Given $\varepsilon > 0$, find pairwise disjoint discs $\{B_j\}$ centered at each vertex and of radius less than ε so that $B_j \cap P$ is connected for each j. Then

$$P \setminus \bigcup_j B_j = \bigcup L_k,$$

where $\{L_k\}$ are pairwise disjoint closed line segments. Cover each L_k with a disc-chain centered on L_k tangent to the corresponding B_j at the ends, and radius less than half the distance to any other L_i, and less than ε.

Another method for constructing a disc-chain is to draw a Jordan curve using only line segments of length 2^{-n} parallel to the coordinate axes. The circles with radius 2^{-n-1} centered at the endpoints of these segments form a disc-chain. The points of
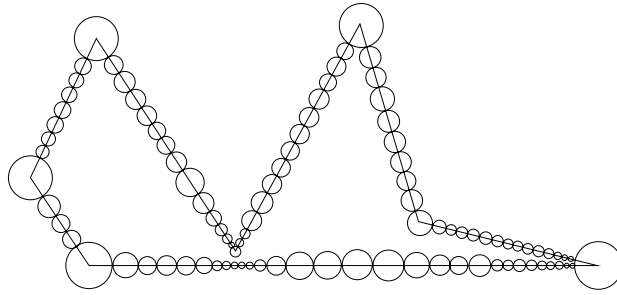
FIG. 7. *Disc-chain covering a polygon.*

tangency are the midpoints of the line segments. Such curves arise from the Whitney decomposition of a simply connected domain, which can be described as follows (see also [GM, p. 21]). If Q is a square, let $2Q$ denote the square with the same center and twice the diameter. Suppose Ω is a simply connected domain contained in the unit square. Divide the unit square into four equal squares.

(a) Discard any square which does not intersect Ω.
(b) If Q is one of the remaining squares for which $2Q \not\subset \Omega$, then divide Q into four equal squares.
(c) Repeat (a), (b), and (c) for the squares obtained in (b).

If this process is repeated ad infinitum, we obtain a decomposition of Ω into squares with the property that for each such square, the distance of the square to the boundary of Ω is comparable to the side length of the square: $2Q \subset \Omega$ and $5Q \cap \partial\Omega \neq \emptyset$. Fix n and $z_0 \in \Omega$ with $\mathrm{dist}(z_0, \partial\Omega) > 2^{-n}$. Let U_n be the union of all squares Q in the Whitney decomposition with side length at least 2^{-n} and let Ω_n be the component of the interior of U_n containing z_0. Then $\partial\Omega_n$ is a polygonal Jordan curve consisting of segments of length 2^{-n}. The discs of radius 2^{-n-1} centered at the endpoints of these segments form a disc-chain and the points of tangency are the midpoints of these segments.

Yet another method for constructing a disc-chain would be to start with a hexagonal grid of tangent discs, all of the same size, and then select a sequence of these discs which form a disc-chain. The boundary circles of a circle packing of a simply connected domain can also be used to form a disc-chain. See, for example, any of the pictures in Stephenson [SK].

If $D_0, D_1, \ldots, D_n$ is a closed disc-chain, set

$$z_j = \partial D_j \cap \partial D_{j+1}$$

for $j = 0, \ldots, n$, where $D_{n+1} \equiv D_0$.

THEOREM 2.2. *If $D_0, D_1, \ldots, D_n$ is a closed disc-chain, then the geodesic algorithm applied to the data $z_0, z_1, \ldots, z_n$ produces a conformal map φ_c^{-1} from the upper-half plane $\mathbb{H}$ to a region bounded by a C^1 and piecewise analytic Jordan curve γ with*

$$\gamma \subset \bigcup_0^n (D_j \cup z_j).$$

Proof. An arc of a circle which is orthogonal to $\mathbb{R}$ is a hyperbolic geodesic in the upper-half plane $\mathbb{H}$. Let γ_j denote the portion of the computed boundary, $\partial\Omega_c$,

between z_j and z_{j+1}. Since hyperbolic geodesics are preserved by conformal maps, γ_j is a hyperbolic geodesic in

$$\mathbb{C}^* \setminus \bigcup_{k=0}^{j-1} \gamma_k.$$

For this reason, we call the algorithm the "geodesic" algorithm.

Using the notation of Figure 2, each map f_a^{-1} is analytic across $\mathbb{R} \setminus \{\pm c\}$, where $f_a^{-1}(\pm c) = 0$, and f_a^{-1} is approximated by a square root near $\pm c$. If f_b^{-1} is another basic map, then f_b^{-1} is analytic and asymptotic to a multiple of z^2 near 0. Thus $f_b^{-1} \circ f_a^{-1}$ preserves angles at $\pm c$. The geodesic γ_j then is an analytic arc which meets γ_{j-1} at z_j with angle π. Thus the computed boundary $\partial \Omega$ is C^1 and piecewise analytic. The first arc γ_0 is a chord of D_0 and hence not tangent to ∂D_0. Since the angle at z_1 between γ_0 and γ_1 is π, γ_1 must enter D_1, and so by Jørgensen's theorem (see Theorem A.1 in the appendix)

$$\gamma_1 \subset D_1,$$

and γ_1 is not tangent to ∂D_1. By induction

$$\gamma_j \subset D_j,$$

$j = 0, 1, \ldots, n$.   □

Disc-chains can be used to approximate the boundary of an arbitrary simply connected domain.

LEMMA 2.3. *Suppose that Ω is a bounded simply connected domain. If $\varepsilon > 0$, then there is a disc-chain $D_0, \ldots, D_n$ so that the radius of each D_j is at most ε and $\partial \Omega$ is contained in an ε-neighborhood of $\bigcup D_j$.*

Proof. We may suppose that Ω is contained in the unit square. Then for n sufficiently large, the disc-chain constructed using the Whitney squares with side length at least 2^{-n}, as described above, satisfies the conclusions of Lemma 2.3.   □

The *Hausdorff distance* d_H in a metric ρ between two sets A and B is the smallest number d such that every point of A is within ρ-distance d of B, and every point of B is within ρ-distance d of A. The ρ-metrics we will consider in this article are the Euclidean and spherical metrics.

A consequence is the following theorem.

THEOREM 2.4. *If Ω is a bounded simply connected domain, then, for any $\varepsilon > 0$, the geodesic algorithm can be used to find a conformal map f_c of $\mathbb{D}$ onto a Jordan region Ω_c so that*

$$(2.1) \qquad\qquad d_H(\partial \Omega, \partial \Omega_c) < \varepsilon,$$

where d_H is the Hausdorff distance in the Euclidean metric. If $\partial \Omega$ is a Jordan curve, then we can find f_c so that

$$\sup_{z \in \mathbb{D}} |f(z) - f_c(z)| < \varepsilon,$$

where f is a conformal map of $\mathbb{D}$ onto Ω.

Proof. The first statement follows immediately from Theorem 2.2 and Lemma 2.3. To prove the second statement, note that the boundary of the regions constructed with
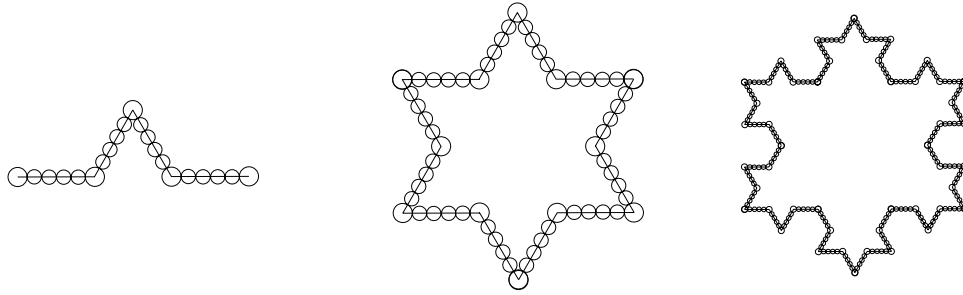
FIG. 8. *Approximating the von Koch snowflake.*

the Whitney decomposition converges to $\partial\Omega$ in the Fréchet sense. By a theorem of Courant [T, p. 383], the mapping functions can be chosen to be uniformly close.   □

We note that if Ω is unbounded, Lemma 2.3 and Theorem 2.4 remain true if we use the spherical metric instead of the Euclidean metric to measure the radii of the discs and the distance to $\partial\Omega$.

There are other ways besides using the Whitney decomposition to approximate the boundary of a region by a disc-chain and hence to approximate the mapping function. However, Theorem 2.4 does not give an explicit estimate of the distance between mapping functions in terms of the geometry of the regions. This issue will be explored in greater detail in sections 4 and 5.

The von Koch snowflake is an example of a simply connected Jordan-domain whose boundary has Hausdorff dimension > 1. The standard construction of the von Koch snowflake provides a sequence of polygons which approximate it (see Figure 8). By Theorem 2.4 the mapping functions constructed from these disc-chains converge uniformly to the conformal map to the snowflake.

It is somewhat amusing and perhaps known that a constructive proof of the Riemann mapping theorem (without the use of normal families) then follows. Using linear fractional transformations and a square root map, we may suppose Ω is a bounded simply connected domain. Using the disc-chains associated with increasing levels of the Whitney decomposition, for instance, Ω can be exhausted by an increasing sequence of domains Ω_n for which the geodesic algorithm can be used to compute the conformal map φ_n of Ω_n onto $\mathbb{D}$ with $\varphi_n(z_0) = 0$ and $\varphi_n'(z_0) > 0$. Then by Schwarz's lemma

$$u_n(w) = \log\left|\frac{\varphi_m(w)}{\varphi_n(w)}\right|$$

for $n = m+1, m+2, \ldots$ is an increasing sequence of positive harmonic functions on Ω_m which is bounded above at z_0 by Schwarz's lemma applied to φ_n^{-1}, since Ω is bounded. By Harnack's estimate u_n is bounded on compact subsets of Ω, and by the Herglotz integral formula, $\log\frac{\varphi_m(w)}{\varphi_n(w)}$ converges uniformly on closed discs contained in Ω_m. Thus φ_n converges uniformly on compact subsets of Ω to an analytic function φ. By Hurwitz's theorem φ is one-to-one. Similarly, $\log|\varphi \circ \varphi_m^{-1}(z)/z|$ is an increasing sequence of negative harmonic functions on $\mathbb{D}$ which tend to 0 at $z = 0$. By Harnack again, $|\varphi \circ \varphi_m^{-1}(z)|$ converges to $|z|$ uniformly on compact subsets of $\mathbb{D}$. If $s < 1$, then $|\varphi \circ \varphi_m^{-1}(z)| > s$ for $|z|$ sufficiently close to 1, so by the argument principle, $\{w : |w| < s\} \subset \varphi(\Omega)$, and since s is arbitrary, $\varphi(\Omega) = \mathbb{D}$.

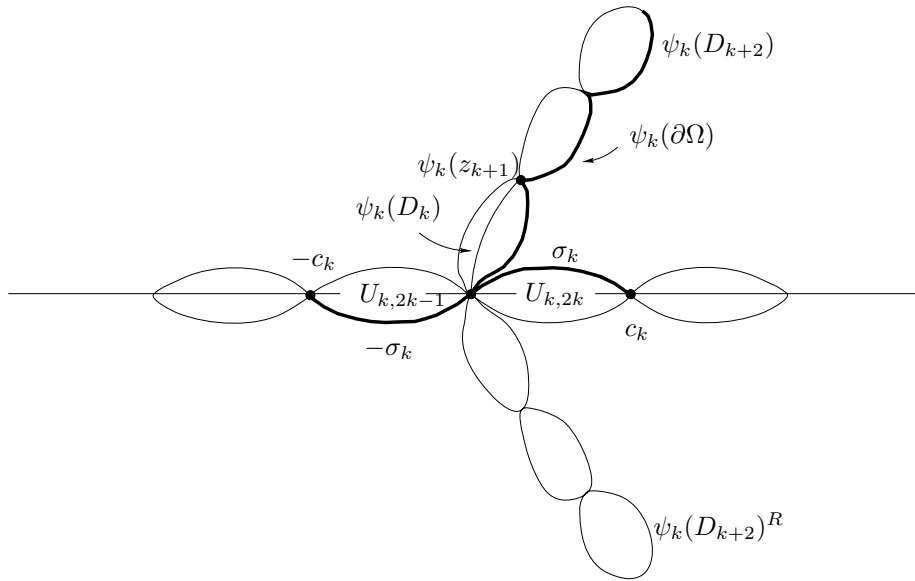In the geodesic algorithm, we have viewed the maps φ_c and φ_c^{-1} as conformal maps

FIG. 9. *Proof of Proposition* 2.5.

between $\mathbb{H}$ and a region Ω_c whose boundary contains the data points. If we are given a region Ω and choose data points $\{z_k\} \in \partial\Omega$ properly, then the next proposition says that the computed maps φ_c and φ_c^{-1} are also conformal maps between the original region Ω and a region "close" to $\mathbb{H}$.

PROPOSITION 2.5. *If $D_0, \ldots, D_n$ is a closed disc-chain with points of tangency $\{z_k\}$, and if Ω is a simply connected domain such that*

$$\partial\Omega \subset \bigcup_{k=0}^{n} \overline{D_k},$$

then the computed map φ_c for the data points $\{z_k\}_0^n$ extends to be conformal on Ω.

We remark that changing the sign of the last map φ_{n+1} in the construction of φ_c gives a conformal map of the complement of the computed region onto $\mathbb{H}$. We choose the sign so that the computed boundary winds once around a given interior point of Ω.

Proof (see Figure 9). Without loss of generality $\Omega \supset \bigcup_{k=0}^{n} D_k$, and hence $\partial\Omega \subset \bigcup \partial D_k$. The basic map f_a in Figure 2 extends by reflection to be a conformal map of $\mathbb{C}^* \setminus (\gamma \cup \gamma^R)$ onto $\mathbb{C}^* \setminus [-c, c]$, where γ^R is the reflection of γ about $\mathbb{R}$. We will first describe the image of $\mathbb{C}^* \setminus \{D_0 \cup \cdots \cup D_n\}$ using these reflected maps. Set

$$\psi_k \equiv \varphi_k \circ \cdots \circ \varphi_1$$

and

$$W_k = \psi_k(\mathbb{C}^* \setminus \{D_0 \cup \cdots \cup D_n\}).$$

Then we claim $\mathbb{C}^* \setminus \{W_k \cup W_k^R\}$ consists of $2(n+1)$ pairwise disjoint simply connected regions:

$$\mathbb{C}^* \setminus \{W_k \cup W_k^R\} = \bigcup_{j=k}^{n} \psi_k(D_j) \cup \psi_k(D_j)^R \cup \bigcup_{j=1}^{2k} U_{k,j},$$

where each region $U_{k,j}$ is symmetric about $\mathbb{R}$ and $\mathbb{R} \subset \bigcup_{j=1}^{2k} \overline{U_{k,j}}$. The case $k = 1$ follows since $\psi_1(\mathbb{C}^* \setminus D_0)$ is bounded by two lines from 0 to ∞. The region $\psi_k(D_k)$ is a subset of $\mathbb{H}$ with 0 and $\psi_k(z_{k+1})$ on its boundary and containing the circular arc from 0 to $\psi_k(z_{k+1})$ which is orthogonal to $\mathbb{R}$. Then

$$\varphi_k\left(\mathbb{C}^* \setminus (\psi_{k-1}(D_{k-1}) \cup \psi_{k-1}(D_{k-1})^R)\right)$$

consists of two regions V and $-V = \{-z : z \in V\}$ with 0 and $c_k \in \partial V \cap \mathbb{R}$ and $-c_k \in \partial(-V) \cap \mathbb{R}$. Set $U_{k,2k} = V$, $U_{k,2k-1} = -V$, and $U_{k,p} = \varphi_k(U_{k-1,p})$ for $p \leq 2k - 2$. The claim now follows by induction.

Finally, we describe the extension of our maps to $\Omega \supset \bigcup_j D_j$. The map φ_k is the composition of a linear fractional transformation τ_k and the map $\sqrt{z^2 + c_k^2}$ (see Figure 2). Note that $\delta_k = \tau_k \circ \psi_{k-1}(\partial\Omega \cap \partial D_{k-1})$ is a curve in $\mathbb{H}$ connecting 0 to ic_k. The map $\sqrt{z^2 + c_k^2}$ is one-to-one and analytic on $\mathbb{C}^* \setminus (\delta_k \cup -\delta_k)$ with image $\mathbb{C}^* \setminus (\sigma_k \cup -\sigma_k)$, where σ_k is a curve connecting 0 to $c_k \in \mathbb{R}$. Thus φ_k extends to be one-to-one and analytic on Ω with image contained in $\mathbb{H} \cup \bigcup_{j=1}^{2k} U_{k,j}$. By induction, ψ_n is one-to-one and analytic on Ω. By direct inspection, the final map φ_{n+1} extends to be one-to-one and analytic, completing the proof of Proposition 2.5.   □

As one might surmise from the proof of Proposition 2.5, care must be taken in any numerical implementation to ensure that the proper branch of $\sqrt{z^2 + c^2}$ is chosen at each stage in order to find the analytic extension of the computed map to all of Ω. For this reason, in the numerical implementation of the geodesic algorithm we define our maps using the right-half plane $\mathbb{H}^+ = \{z : \operatorname{Re} z > 0\}$ instead of $\mathbb{H}$.

3. Diamond-chains and pacmen. If we have more control than the disc-chain condition on the behavior of the boundary of a region, then we show in this section that the geodesic algorithm approximates the boundary with better estimates. The computed curve always has a continuously turning tangent direction. The goal in this section is to show that if enough data points are taken on a C^1 Jordan curve, then not only is the computed curve uniformly close, but also the tangent directions are uniformly close to the tangent directions of the given curve. If a subcollection $z_k, z_{k+1}, \ldots, z_p$ of the data points all lie along a line segment, then it is conceivable that the computed curve passing through the data points is oscillating alternately up and down between the data points, and then if z_{p+1} is off the line, it could conceivably cause subsequent oscillations to worsen. Over the long run, the oscillations might then become so large that the curve is no longer a C^1 approximation to the given curve. The key lemma, Lemma 3.5 below, shows that the tangent direction at the end of the geodesic arc actually improves if z_{p+1} is not too far from the line. It is this fixed fractional improvement which does not depend on the number of data points that allows us to iterate the argument.

We will first restrict our attention to domains of the form $\mathbb{C} \setminus \gamma$, where γ is a Jordan arc tending to ∞.

DEFINITION 3.1. *An ε-diamond $D(a,b)$ is an open rhombus with opposite vertices a and b and interior angle 2ε at a and at b. If $a = \infty$, then an ε-diamond $D(\infty, b)$ is a sector $\{z : |\arg(z - b) - \theta| < \varepsilon\}$. An ε-diamond-chain is a pairwise disjoint sequence of ε-diamonds $D(z_0, z_1), D(z_1, z_2), \ldots, D(z_{n-1}, z_n)$. A closed ε-diamond-chain is an ε-diamond-chain with $z_n = z_0$.*

See Figure 10. Let $B(z, R)$ denote the disc centered at z with radius R.

DEFINITION 3.2. *A pacman is a region of the form*

$$P = B(z_0, R) \setminus \{z : |\arg(\overline{\lambda}(z - z_0))| \leq \varepsilon\}$$
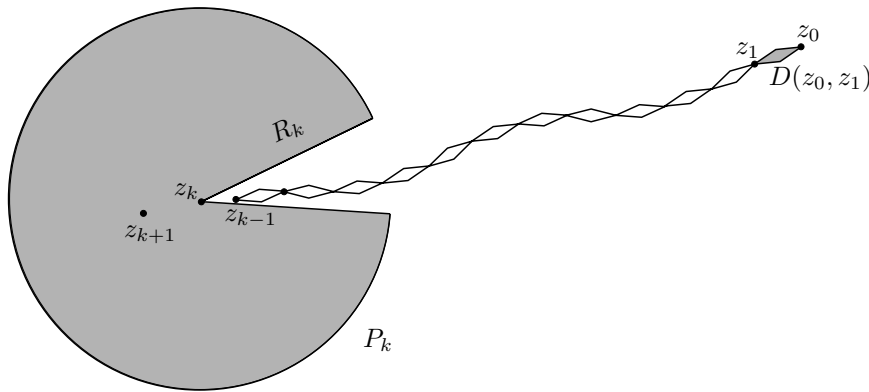
FIG. 10. *A diamond-chain and a pacman.*

for some radius $R < \infty$, center z_0, opening $2\varepsilon > 0$, *and* rotation λ, $|\lambda| = 1$.

Let C_1 be a constant to be chosen later (see Lemma 3.7), and let $z_0 = \infty$.

DEFINITION 3.3. *An ε-diamond-chain* $D(\infty, z_1), D(z_1, z_2), \ldots, D(z_{n-1}, z_n)$ *satisfies the ε-pacman condition if for each* $1 \leq k \leq n-1$ *the pacman*

$$P_k = B(z_k, R_k) \setminus \left\{ z : \left| \arg\left(\frac{z - z_k}{z_k - z_{k+1}} \right) \right| \leq \varepsilon \right\}$$

with radius $R_k = C_1 |z_{k+1} - z_k| / \varepsilon^2$ *satisfies*

$$\left(\bigcup_{j=0}^{k-2} D(z_j, z_{j+1}) \right) \cap P_k = \emptyset.$$

The pacman P_k in Definition 3.3 is chosen to be symmetric about the segment between z_k and z_{k+1} with opening 2ε equal to the interior angle 2ε in the diamond-chain. Note that the ε-diamond $D(z_{k-1}, z_k)$ may intersect P_k.

The pacman condition is a quantitative method of estimating how "flat" the polygonal curve through the data points is and prevents the data point z_k from being too close to z_p for larger p (relative to $|z_k - z_{k+1}|$), as might happen if the polygon almost folded back onto itself as in Figure 7. The requirement is more stringent than the disc-chain condition, and it will allow us to control the smoothness of the unit tangent vector on the boundary of the computed region. If we start with a C^1 curve, then we can select data points that satisfy the pacman condition by making the spacing between successive data points smaller in places where the tangent vector is changing rapidly and where the curve almost folds back on itself.

When $z_0 = \infty$, the first map in the geodesic algorithm is replaced by $\varphi_1(z) = \lambda\sqrt{z - z_1}$. The argument of λ can be chosen so that $\varphi_1(z_2)$ is purely imaginary, in which case the boundary of the constructed region contains the half line from z_2 through z_1 and ∞. We will henceforth assume that

$$D(\infty, z_1) = \left\{ z : \left| \arg\left(\frac{z - z_1}{z_1 - z_2} \right) \right| < \varepsilon \right\}.$$

THEOREM 3.4. *There exist universal constants* $\varepsilon_0 > 0$ *and* C_1 *such that if an ε-diamond-chain*

$$D(\infty, z_1), D(z_1, z_2), \ldots, D(z_{n-1}, z_n)$$

satisfies the ε-pacman condition with $\varepsilon < \varepsilon_0$, and if

(3.1)
$$\left| \arg \left(\frac{z_{k+1} - z_k}{z_k - z_{k-1}} \right) \right| < \frac{\varepsilon}{10}$$

for $k = 2, \ldots, n-1$, then the boundary curve γ_c computed by the geodesic algorithm with the data $z_0 = \infty, z_1, \ldots, z_n$ satisfies

$$\gamma_c \subset \bigcup_{k=1}^{n} \left(D(z_{k-1}, z_k) \cup \{z_k\} \right).$$

Moreover, the argument θ of the tangent to γ_c between z_k and z_{k+1} satisfies

$$|\theta - \arg(z_{k+1} - z_k)| < 3\epsilon.$$

To prove Theorem 3.4, we first give several lemmas. To understand the motivation for the lemmas, perhaps it is helpful to point out that the computed boundary $\partial\Omega$ has a smoothly turning tangent, so that if $\gamma_j \subset D(z_j, z_{j+1})$ were tangent to $\partial D(z_j, z_{j+1})$ at z_{j+1}, then, if z_{j+2} were even slightly off the continuation of the straight line from z_j to z_{j+1} (on one side), γ_{j+1} would not be contained in $D(z_{j+1}, z_{j+2})$. This is why we need the improvement provided by the lemmas.

LEMMA 3.5. *There exists $\varepsilon_0 > 0$ such that if $\varepsilon < \varepsilon_0$, and if Ω is a simply connected region bounded by a Jordan arc $\partial\Omega$ from 0 to ∞ with*

$$\{z : |\arg z| < \pi - \varepsilon\} \subset \Omega,$$

then the conformal map f of $\mathbb{H}^+ = \{z : \operatorname{Re} z > 0\}$ onto Ω normalized so that $f(0) = 0$ and $f(\infty) = \infty$ satisfies

(3.2)
$$|\arg z_0^2 f'(z_0)| < \frac{5\varepsilon}{6},$$

where $z_0 = f^{-1}(1)$.

The circle C_{z_0}, which is orthogonal to the imaginary axis at 0 and passes through z_0, has a tangent vector at z_0 with argument equal to $2 \arg z_0$. The quantity $\arg z_0^2 f'(z_0)$ in (3.2) is the argument of the tangent vector to $f(C_{z_0})$ at $f(z_0)$.

Proof. We may suppose that $|z_0| = 1$. Set

$$g(z) = \log \frac{f(z)}{z^2}.$$

Then $|\operatorname{Im} g(z)| \leq \varepsilon$ on $\partial\mathbb{H}^+$ and hence also on $\mathbb{H}^+$, and $|\arg z_0| \leq \frac{\varepsilon}{2}$, since $f(z_0) = 1$. Set $\alpha = \frac{\pi}{2\varepsilon}$ and

$$A = e^{\alpha g(z_0)} = z_0^{-2\alpha},$$

$$\varphi(z) = \frac{e^{\alpha z} - A}{e^{\alpha z} + \overline{A}},$$

and

$$\tau(z) = \frac{1+z}{1-z} \operatorname{Re} z_0 + i \operatorname{Im} z_0.$$

Then τ is a conformal map of $\mathbb{D}$ onto $\mathbb{H}^+$ such that $\tau(0) = z_0$ and φ is a conformal map of the strip $\{|\operatorname{Im} z| < \varepsilon\}$ onto $\mathbb{D}$ so that $\varphi(g(z_0)) = 0$. Thus $h = \varphi \circ g \circ \tau$ is analytic on $\mathbb{D}$ and bounded by 1 and $h(0) = 0$, so that by Schwarz's lemma

$$|\varphi'(g(z_0))|\,|g'(z_0)|\,|\tau'(0)| = |h'(0)| \le 1.$$

Consequently

$$\left| \frac{f'(z_0)}{f(z_0)} - \frac{2}{z_0} \right| = |g'(z_0)| \le \frac{2\varepsilon|\operatorname{Re} A|}{\pi \operatorname{Re} z_0} \le \frac{2\varepsilon}{\pi \cos \frac{\varepsilon}{2}},$$

and hence

$$
\begin{aligned}
|\arg z_0^2 f'(z_0)| &= \left| \arg z_0 + \arg \frac{z_0 f'(z_0)}{f(z_0)} \right| \\
&\le \frac{\varepsilon}{2} + \sin^{-1}\left(\frac{\varepsilon}{\pi \cos \frac{\varepsilon}{2}} \right) \\
&= \left(\frac{1}{2} + \frac{1}{\pi} \right) \varepsilon + \mathrm{O}(\varepsilon^2).
\end{aligned}
$$

This proves Lemma 3.5 if ε is sufficiently small.   □

LEMMA 3.6. *Let Ω satisfy the hypotheses of Lemma 3.5. If $\varepsilon < \varepsilon_0/2$, then the hyperbolic geodesic γ from 0 to 1 for the region Ω lies in the kite*

$$P = \left\{ z : |\arg z| < \varepsilon \right\} \cap \left\{ z : |\arg(1 - z)| < \frac{5\varepsilon}{6} \right\},$$

and the tangent vectors to γ have argument less than $\frac{8}{3}\varepsilon$.

Proof. By Jørgensen's theorem, γ is contained in the closed disc through 1 and 0 which has slope $\tan \varepsilon$ at 0. Likewise γ is contained in the reflection of this disc about $\mathbb{R}$, and hence $|\arg z| < \varepsilon$ on γ. This also shows that γ is contained in a kite like P but with angles ε at both 0 and 1. In the proof of Theorem 3.4, however, we need the improvement to $\frac{5\varepsilon}{6}$ of the angle at 1.

By Lemma 3.5, a portion of γ near 1 lies in P. Suppose $w_1 \in \gamma$ with $|\arg w_1| = \delta < \varepsilon$ and then apply Lemma 3.5 to the region $\frac{1}{w_1}\Omega$ with ε replaced by $\varepsilon + \delta$. Then the tangent vector to γ at w_1 has argument θ, where

(3.3) $$|\theta - \arg w_1| < \frac{5}{6}(\varepsilon + |\arg w_1|).$$

Since $|\arg w_1| < \varepsilon$, we have $|\theta| \le \frac{8}{3}\varepsilon$. Moreover, (3.3) also implies $\theta < \frac{5}{6}\varepsilon$ when $\arg w_1 \le 0$ and $\theta > -\frac{5}{6}\varepsilon$ when $\arg w_1 \ge 0$. But if w_1 is the last point on $\gamma \cap \partial P$ before reaching 1, this is impossible. Thus $\gamma \subset P$, proving the lemma.   □

The next lemma improves Lemma 3.5 by requiring only that the portion of $\partial\Omega$ in a large disc lies inside a small sector.

LEMMA 3.7. *There is a constant C_1 so that if $\varepsilon < \varepsilon_0/2$ and if $\partial\Omega$ is a Jordan arc such that $0 \in \partial\Omega$, $\partial\Omega \cap \{|z| > C_1/\varepsilon^2\} \ne \emptyset$, and*

$$P_\varepsilon = \left\{ z : |\arg z| < \pi - \varepsilon \text{ and } |z| \le \frac{C_1}{\varepsilon^2} \right\} \subset \Omega,$$

then the conformal map $f : \mathbb{H}^+ \longrightarrow \Omega$ with $f(0) = 0$ and $|f(\infty)| > \frac{C_1}{\varepsilon^2}$ satisfies

(3.4) $$|\arg z_0^2 f'(z_0)| < \frac{9\varepsilon}{10},$$

where $z_0 = f^{-1}(1)$.

Proof. Set $R = \frac{C_1}{\varepsilon^2}$ and $B_R = B(0, R) = \{|z| < R\}$. Let U_R be the component of $\Omega \cap B_R$ containing the point 1. Then $f^{-1}(U_R) \subset \mathbb{H}^+$ is bounded by a set $F \subset i\mathbb{R}$ and curves $\sigma_j \subset \mathbb{H}^+$ on which $|f| = R$. Since $0 \in \partial f^{-1}(U_R)$ and $f(\infty) \notin B_R$, exactly one of the curves (call it σ_1) will connect the positive imaginary axis to the negative imaginary axis. The function $u(z) = \arg f(z) - \arg z^2$ is harmonic on the simply connected region $f^{-1}(U_R)$ with $|u| \le 2\pi + \varepsilon$. Then $\partial\Omega \cap B_R$ contains a subarc δ connecting 0 to ∂B_R and $|u| < \varepsilon$ on $f^{-1}(\delta)$. It is possible that B_R contains other subarcs of $\partial\Omega$, none of which intersect P_ε. We may suppose that $P_\varepsilon \cap \partial B_R \subset f(\sigma_1)$, for if $P_\varepsilon \cap \partial B_R \subset f(\sigma_j)$, $j \ne 1$, then σ_j separates a point $z_1 \in i\mathbb{R}$ from $f^{-1}(U_R)$. Then

$$g(\zeta) = f\left(\frac{\zeta}{1 + \zeta/z_1}\right)$$

satisfies the hypotheses of the lemma and $P_\varepsilon \cap \partial B_R$ is a subset of the image of the corresponding curve in $\mathbb{H}^+$ connecting the positive and negative imaginary axes. Moreover, a direct computation shows that

$$\zeta_0^2 g'(\zeta_0) = z_0^2 f'(z_0),$$

where $\zeta_0 = z_0/(1 - z_0/z_1)$.

We conclude $|u(z)| < \varepsilon$ at the endpoints of each σ_j because $P_\varepsilon \subset U_R$. Since u is continuous on the closure of $f^{-1}(U_R)$, and $|\arg f| > \pi - \varepsilon$ on $\partial f^{-1}(U_R) \cap i\mathbb{R}$, and $\arg z^2$ is the same at each endpoint of σ_j, $j > 1$, we conclude that $|u| < \varepsilon$ on $\partial f^{-1}(U_R) \cap i\mathbb{R}$. By the maximum principle

$$|u(z)| \le \varepsilon + (2\pi + \varepsilon)\omega(f(z), \partial B_r, U_R)$$

for $z \in f^{-1}(U_R)$, where $\omega(z, E, V)$ is the harmonic measure at z for $E \cap \overline{V}$ in $V \setminus E$. By Beurling's projection theorem [GM, p. 105] and a direct computation (see [GM, Corollary III.9.3])

$$(3.5) \qquad \omega(1, \partial B_R, \Omega) \le \omega(1, \partial B_R, B_R \setminus [-R, 0]) = \frac{4}{\pi} \tan^{-1}\left(\frac{1}{R^{\frac{1}{2}}}\right).$$

Evaluating at $z_0 = f^{-1}(1)$, we obtain

$$|u(z_0)| = |-\arg z_0^2| \le \varepsilon + (2\pi + \varepsilon)\frac{4}{\pi}\tan^{-1}\left(\frac{\varepsilon}{C_1^{\frac{1}{2}}}\right) < \frac{11\varepsilon}{10}$$

for C_1 sufficiently large. Thus

$$(3.6) \qquad\qquad\qquad |\arg z_0| \le \frac{11\varepsilon}{20}.$$

Next we show that there is a large half disc contained in $f^{-1}(\Omega \cap B_R)$. We may suppose that $|z_0| = 1$. Set

$$S = \inf\{|w - i\operatorname{Im} z_0| : w \in \mathbb{H}^+ \text{ and } f(w) \in \partial B_R\}.$$

Using the map

$$\frac{z - i\operatorname{Im} z_0 - S}{z - i\operatorname{Im} z_0 + S}$$

of $\mathbb{H}^+$ onto $\mathbb{D}$ and Beurling's projection theorem again,

$$\omega(z_0, f^{-1}(\partial B_R), \mathbb{H}^+) \geq \omega(z_0, [S, \infty) + i \operatorname{Im} z_0, \mathbb{H}^+).$$

Then by (3.5), (3.6), and an explicit computation

$$\frac{4}{\pi} \tan^{-1}\left(\frac{\varepsilon}{C_1^{\frac{1}{2}}}\right) \geq \frac{2}{\pi} \tan^{-1}\left(\frac{\operatorname{Re} z_0}{\sqrt{S^2 - \operatorname{Re} z_0^2}}\right).$$

For ε sufficiently small, this implies

$$B\left(0, \frac{C_1^{\frac{1}{2}}}{2\varepsilon}\right) \cap \mathbb{H}^+ \subset f^{-1}\left(\Omega \cap B\left(0, \frac{C_1}{\varepsilon^2}\right)\right).$$

Now follow the proof of Lemma 3.5 replacing τ with a conformal map of $\mathbb{D}$ onto $\mathbb{H}^+ \cap \{|z| < \frac{C_1^{1/2}}{2\varepsilon}\}$ such that $\tau(0) = z_0$. Then $\tau'(0) = 2 \operatorname{Re} z_0 + O(\frac{\varepsilon}{C_1^{1/2}})$, and for C_1 sufficiently large, (3.4) holds.   □

Following the proof of Lemma 3.6 (replacing 5/6 by 9/10), the next corollary is obtained.

COROLLARY 3.8. *Suppose $\partial\Omega$ is a Jordan arc such that $0 \in \partial\Omega$, $\partial\Omega \cap \{|z| > C_1/\varepsilon^2\} \neq \emptyset$, and*

$$\left\{z : |\arg z| < \pi - \varepsilon \text{ and } |z| \leq \frac{C_1}{\varepsilon^2}\right\} \subset \Omega.$$

If $\varepsilon < \varepsilon_0/2$, then the hyperbolic geodesic γ from 0 to 1 for the region Ω lies in the kite

$$(3.7) \qquad P = \{z : |\arg z| \leq \varepsilon\} \cap \left\{z : |\arg(1 - z)| \leq \frac{9\varepsilon}{10}\right\}.$$

Moreover, the tangent vectors to this geodesic have argument at most 3ε.

Proof of Theorem 3.4. Use the constant C_1 from Lemma 3.7 in Definition 3.3. As in Theorem 2.2, let γ_j denote the portion of the computed boundary $\partial\Omega_c$ between z_j and z_{j+1}. By construction $\gamma_0 \cup \gamma_1$ is a half line through $z_0 = \infty$, z_1, and z_2. Make the inductive hypotheses that

$$(3.8) \qquad \bigcup_{j=0}^{k-1} \gamma_j \subset \bigcup_{j=0}^{k-1} D(z_j, z_{j+1})$$

and

$$(3.9) \qquad \gamma_{k-1} \cap P_k = \emptyset.$$

Since the ε-diamond-chain $D(\infty, z_1), D(z_1, z_2), \ldots, D(z_{n-1}, z_n)$ satisfies the ε-pacman condition, (3.8) and (3.9) show that the hypotheses of Corollary 3.8 hold for the curve $\gamma = \bigcup_0^{k-1} \gamma_j$ and hence $\gamma_k \subset D(z_k, z_{k+1})$. Also, by Corollary 3.8 and (3.1),

$$\gamma_k \cap P_{k+1} = \emptyset.$$

By induction, the theorem follows.   □

If the hypotheses of Theorem 3.4 hold, then the proof of Proposition 2.5 gives the following corollary.

COROLLARY 3.9. *If Ω and the diamond-chain $D(z_k, z_{k+1})$ satisfy the hypotheses of Theorem 3.4, then the conformal map φ_c computed in the geodesic algorithm extends to be conformal on $\Omega \cup \bigcup_{k=0}^{n} D(z_k, z_{k+1})$.*

The next theorem says that for a region Ω bounded by a C^1 curve, the geodesic algorithm with data points $z_0, z_1, \ldots, z_n$ produces a region Ω_c whose boundary is a C^1 approximation to $\partial \Omega$.

THEOREM 3.10. *Suppose Ω is a Jordan region bounded by a C^1 curve $\partial \Omega$. Then there exists $\delta_0 > 0$ depending on $\partial \Omega$ so that for $\delta < \delta_0$,*

$$\partial \Omega \subset \bigcup_k \left(D(z_k, z_{k+1}) \cup \{z_k\} \right),$$

where $D = \bigcup D(z_k, z_{k+1})$ is a δ-diamond-chain, and so that $\partial \Omega_c$, the boundary of the region computed by the geodesic algorithm, is contained in $D \cup (\bigcup_k \{z_k\})$. Moreover, if $\zeta \in \partial \Omega_c$ and if $\alpha \in \partial \Omega$ with $|\zeta - \alpha| < \delta$, then

$$(3.10) \qquad |\eta_\zeta - \eta_\alpha| < 6\delta,$$

where η_ζ and η_α are the unit tangent vectors to $\partial \Omega$ and $\partial \Omega_c$ at ζ and α, respectively.

Proof. There were two reasons for requiring that $z_0 = \infty$ in Theorem 3.4. The first reason was to ensure that

$$(3.11) \qquad \left(\bigcup_0^{k-1} \gamma_j \right) \cap (\mathbb{C} \setminus B(z_k, R_k)) \neq \emptyset,$$

as needed for Lemma 3.7. The second reason is the difficulty in closing the curve, since Lemma 3.7 does not apply. The difficulty is that a pacman centered at z_n will contain z_0 if z_0 is too close to z_n. Since $\partial \Omega \in C^1$, we may suppose that the δ-diamond-chain $D(z_0, z_1), D(z_1, z_2), \ldots, D(z_{n-1}, z_n)$ satisfies the pacman condition. Note that this requires z_n to be much closer to z_{n-1} than to z_0. Since $\partial \Omega \in C^1$, if $|z_n - z_0|$ is sufficiently small, we can find two discs

$$\Delta_p \subset \mathbb{C} \setminus \bigcup_0^{n-1} D(z_k, z_{k+1})$$

for $p = 1, 2$ with

$$\{z_0, z_n\} = \partial \Delta_1 \cap \partial \Delta_2 \quad \text{and} \quad \Delta_1 \cap \Delta_2 \subset D(z_n, z_0),$$

where $D(z_n, z_0)$ is a δ-diamond. By Jørgensen's theorem, as in the proof of Theorem 2.2, the geodesic γ_n between z_n and z_0 is contained in $\Delta_1 \cap \Delta_2$. Then by the proof of Theorem 3.4, $\partial \Omega_c$ is contained in the δ-diamond-chain. The statement about tangent vectors now follows from Corollary 3.8.   □

We say that $\{z_k\}$ are *locally evenly spaced* if

$$(3.12) \qquad \frac{1}{D} \leq \left| \frac{z_k - z_{k-1}}{z_k - z_{k+1}} \right| \leq D$$

for some constant $D < \infty$. Note that the spacing between points can still grow or decay geometrically. We define the *mesh size μ* of the data points $\{z_j\}$ to be

$$\mu(\{z_j\}) = \sup_k |z_k - z_{k+1}|.$$

We say that a Jordan curve Γ in the extended plane $\mathbb{C}^*$ is a K-*quasicircle* if for some linear fractional transformation τ

$$(3.13) \qquad \frac{|w_1 - w| + |w - w_2|}{|w_1 - w_2|} \le K$$

for all $w_1, w_2 \in \tau(\Gamma)$ and for all w on the subarc of $\tau(\Gamma)$ with smaller diameter. Thus circles and lines are 1-quasicircles. Quasicircles look very flat on all scales if K is close to 1, but for any $K > 1$ they can contain a dense set of spirals. See, for example, Figure 8.

If Γ satisfies (3.13) with $K = 1 + \delta$ and small δ and if $\{z_k\} \subset \tau(\Gamma)$ is locally evenly spaced, then

$$(3.14) \qquad \left| \arg\left(\frac{z_k - z_{k-1}}{z_{k+1} - z_k} \right) \right| \le C\delta^{\frac{1}{2}}$$

for some constant C, depending on D. The referee suggested that a proof of this fact might help the reader. Note that (3.12), (3.13), and (3.14) are invariant under translations and dilations, so that we may assume $z_{k-1} = -1$ and $z_k = 0$ and write $z_{k+1} = \zeta$. Then (3.13), with $w_1 = -1$, $w = 0$, and $w_2 = \zeta$, shows that

$$1 + |\zeta| \le (1 + \delta)|1 + \zeta|.$$

Writing $\zeta = re^{i\theta}$ and squaring yield

$$1 - \cos\theta \le (2\delta + \delta^2)\frac{(1 + r)^2}{2r}.$$

By (3.12) $D^{-1} \le |\zeta| = r \le D$ so that

$$\frac{\theta^2}{2} \le (2\delta + \delta^2)\frac{(1 + D)^2}{2D},$$

and

$$\left| \arg\left(\frac{z_k - z_{k-1}}{z_{k+1} - z_k} \right) \right| = |\theta| \le C\delta^{\frac{1}{2}}.$$

THEOREM 3.11. *There is a constant $K_0 > 1$ so that if Γ is a K-quasicircle with $K = 1 + \delta < K_0$ and if $\{z_k\}$ are locally evenly spaced on Γ, then the geodesic algorithm finds a conformal map of $\mathbb{H}$ onto a region Ω_c bounded by a $C(K)$-quasicircle containing the data points $\{z_k\}$, where $C(K)$ is a constant depending only on K.*

We can choose $C(K)$ so that $C(K) \to 1$ as $K \to 1$. Moreover, given $\eta > 0$, if the mesh size $\mu(\{z_k\})$ is sufficiently small, then

$$d_H(\Gamma, \partial\Omega_c) < \eta,$$

where d_H is the Hausdorff distance in the spherical metric.

Proof. We may suppose that Γ satisfies (3.13) with $K = 1 + \delta$ and δ small. Note that $\infty \in \Gamma$. If $\{z_k\}_1^n$ are locally evenly spaced points on $\partial\Omega$, with $\mu = \max|z_k - z_{k-1}|$ sufficiently small, then (3.14) holds and $D(\infty, z_1), D(z_1, z_2), \ldots, D(z_{n-1}, z_n), D(z_n, \infty)$ is a $C\delta^{\frac{1}{2}}$-diamond-chain, where the main axis of the cone $D(\infty, z_1)$ is in the direction $z_1 - z_2$ and the main axis of $D(z_n, \infty)$ is in the direction $z_n - z_{n-1}$. Moreover, $D(\infty, z_1), D(z_1, z_2), \ldots, D(z_{n-1}, z_n)$ satisfies the ε-pacman condition if

$$\varepsilon \ge C\delta^{\frac{1}{4}}$$

for some universal constant C. Now apply Theorem 3.4 to obtain $\gamma_j \subset D(z_{j-1}, z_j)$, $j = 1, \ldots, n-1$. By an argument similar to the proof of Theorem 3.10, we can also find a geodesic arc for $\mathbb{C} \setminus (\bigcup_0^{n-1} \gamma_j)$ from z_n to ∞ contained in $D(z_n, \infty)$. Then the computed curve will be a $C(K)$-quasicircle.

Note that if w_1, w, and w_2 are data points, then by assumption (3.13) holds with $K = 1 + \delta$. By Corollary 3.8, the tangent directions to the computed curve change by no more than $C\delta^{\frac{1}{4}}$ between the data points, and hence the computed curve is a $(1 + C'\delta^{\frac{1}{4}})$-quasicircle. $\square$

As noted before, the boundary of the region computed with the geodesic algorithm, $\partial\Omega_c$, is a C^1 curve. We end this section by proving that $\partial\Omega_c$ is slightly better than C^1. If $0 < \alpha < 1$, we say that a curve Γ *belongs to* $C^{1+\alpha}$ if arc length parameterization $\gamma(s)$ of Γ satisfies

$$|\gamma'(s_1) - \gamma'(s_2)| \leq C|s_1 - s_2|^\alpha$$

for some constant $C < \infty$.

We say that a conformal map f defined on a region Ω *belongs to* $C^{1+\alpha}(\overline{\Omega})$, $0 < \alpha < 1$, provided f and f' extend to be continuous on $\overline{\Omega}$ and there is a constant C so that

$$|f'(z_1) - f'(z_2)| \leq C|z_1 - z_2|^\alpha$$

for all z_1, z_2 in $\overline{\Omega}$.

PROPOSITION 3.12. *If the bounded Jordan region Ω_c is the image of the unit disc by the geodesic algorithm, then*

$$\partial\Omega_c \in C^{3/2},$$

and $\partial\Omega_c \notin C^{1+\alpha}$ for $\alpha > 1/2$, unless Ω_c is a circle or a line. Moreover, $\varphi \in C^{3/2}(\overline{\Omega_c})$ and $\varphi^{-1} \in C^{3/2}(\overline{\mathbb{D}})$.

Proof. To prove the first statement, it is enough to show that if γ is an arc of a circle in $\mathbb{H}$ which meets $\mathbb{R}$ orthogonally at 0 (constructed by application of one of the maps f_a^{-1} as in Figure 2), then the curve σ which is the image of $[-1, 1] \cup \gamma$ by the map $S(z) = \sqrt{z^2 - d^2}$ is $C^{\frac{3}{2}}$ (and no better class) in a neighborhood of $S(0) = id$. Indeed, subsequent maps in the composition φ^{-1} are conformal in $\mathbb{H}$ and hence preserve smoothness. For $d > 0$, the function

$$\psi(z) = \sqrt{\left(\frac{\sqrt{z^2 - c^2}}{1 + \sqrt{z^2 - c^2}/b}\right)^2 - d^2} = id + \frac{i}{2d}(z^2 - c^2) - \frac{i}{bd}(z^2 - c^2)^{\frac{3}{2}} + \mathrm{O}((z^2 - c^2)^2)$$

for some choice of $b \in \mathbb{R}$ and $c > 0$ is a conformal map of the upper-half plane onto a region whose complement contains the curve σ. Clearly $\psi \in C^{\frac{3}{2}}$ near $z = \pm c$, and so by a theorem of Kellogg (see [GM, p. 62]), $\sigma \in C^{\frac{3}{2}}$. The same theorem implies σ is not in C^α for $\alpha > \frac{3}{2}$ unless $1/b = 0$. This argument also shows that $\varphi_c \in C^{3/2}(\overline{\Omega})$. To prove $\varphi_c^{-1} \in C^{\frac{3}{2}}(\overline{\mathbb{D}})$, apply the same ideas above to the inverse maps. Alternatively, this last fact can be proved by following the proof of Lemma II.4.4 in [GM]. $\square$

4. Estimates for conformal maps onto nearby domains. We begin this section with a discussion of the following question. Consider two simply connected planar domains Ω_j with $0 \in \Omega_j$ and conformal maps $\varphi_j : \Omega_j \to \mathbb{D}$ fixing 0, suitably normalized (for instance, positive derivative at 0). If Ω_1 and Ω_2 are "close," what can
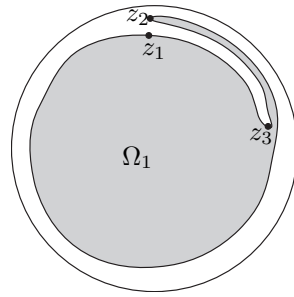
FIG. 11. *Small Hausdorff distance.*

be said about $|\varphi_1 - \varphi_2|$ on $\Omega_1 \cap \Omega_2$, or about $|\varphi_1^{-1} - \varphi_2^{-1}|$ on $\mathbb{D}$? The article [W] gives an overview and numerous results in this direction. How should "closeness" of the two domains be measured? Simple examples show that the Hausdorff distance in the Euclidean or spherical metric between the boundaries does not give uniform estimates for either $||\varphi_1 - \varphi_2||_\infty$ or $||\varphi_1^{-1} - \varphi_2^{-1}||_\infty$. For example, in Figure 11, Ω_1 contains a disc of radius $1 - \delta$, where δ is small, and hence for $\Omega_2 = \mathbb{D}$, $d_H(\Omega_1, \Omega_2) \leq \delta$, but $|\varphi_1(z_1) - \varphi_1(z_2)|$ is large and $|\varphi_1(z_2) - \varphi_1(z_3)|$ is small so that neither $||\varphi_1(z) - z||_\infty$ nor $||\varphi_1^{-1}(z) - z||_\infty$ is small.

Mainly for ease of notation, we will assume throughout this section that the Ω_j are Jordan-domains, and denote by $\gamma_j : \partial\mathbb{D} \to \partial\Omega_j$ an orientation preserving parameterization. Even the more refined distance

$$\inf_\alpha ||\gamma_1 - \gamma_2 \circ \alpha||_\infty,$$

where the infimum is over all homeomorphisms α of $\partial\mathbb{D}$, does not control $||\varphi_1^{-1} - \varphi_2^{-1}||_\infty$ or $||\varphi_1 - \varphi_2||_\infty$. For example, let Ω_2 be a small rotation of the region Ω_1 in Figure 11. What is needed is some control on the "roughness" of the boundary. Following [W], for a simply connected domain Ω we define

$$\eta(\delta) = \eta_\Omega(\delta) = \sup_C \operatorname{diam} T(C),$$

where the supremum is over all crosscuts of Ω with $\operatorname{diam} C \leq \delta$, and where $T(C)$ is the component of $\Omega \setminus C$ that does not contain 0. Notice that $\eta(\delta) \to 0$ as $\delta \to 0$ is equivalent to saying that $\partial\Omega$ is locally connected, and the condition $\eta(\delta) \leq K\delta$ for some constant K is equivalent to saying that Ω is a John-domain (see, e.g., [P, Chapter 5]). It is not difficult to control the modulus of continuity of $\varphi^{-1} : \mathbb{D} \to \Omega$ in terms of η; see [W, Theorem I]. This can be used to estimate $||\varphi_1^{-1} - \varphi_2^{-1}||_\infty$ in terms of the Hausdorff distance between the boundaries, for example.

THEOREM 4.1 (Warschawski [W, Theorem VI]). *If Ω_1 and Ω_2 are John-domains, $\eta_j(\delta) \leq \kappa\delta$ for $j = 1, 2$, and if $d_H(\partial\Omega_1, \partial\Omega_2) \leq \epsilon$, then*

$$||\varphi_1^{-1} - \varphi_2^{-1}||_\infty \leq C\epsilon^\alpha$$

with $\alpha = \alpha(\kappa)$ and $C = C(\kappa, \operatorname{dist}(0, \partial\Omega_1 \cup \partial\Omega_2))$.

In fact, Warschawski proves that every $\alpha < 2/(\pi^2\kappa^2)$ will work (with $C = C(\alpha)$). Using the Hölder continuity of quasiconformal maps, his proof can easily be modified to give the following better estimate if Ω_1 and Ω_2 are K-quasidiscs with K near 1. A K-quasidisc is a Jordan region bounded by a K-quasicircle.

COROLLARY 4.2. *If Ω_1 and Ω_2 are K-quasidiscs, and if $d_H(\partial\Omega_1, \partial\Omega_2) \le \epsilon$, then*

$$||\varphi_1^{-1} - \varphi_2^{-1}||_\infty \le C\epsilon^\alpha$$

with $\alpha = \alpha(K) \to 1$ as $K \to 1$.

As for estimates of $||\varphi_1 - \varphi_2||_\infty$, Warschawski shows [W, Theorem VII] that

$$\sup_{\Omega_1} |\varphi_1 - \varphi_2| \le C\epsilon^{1/2} \log \frac{2}{\epsilon}$$

if $\Omega_1 \subset \Omega_2$ and if Ω_1 is a John-domain, with C depending on κ and on $\operatorname{dist}(0, \partial\Omega_1 \cup \partial\Omega_2)$. However, his result does not apply without the assumption of inclusion $\Omega_1 \subset \Omega_2$. To treat the general case the trick of controlling $|\varphi_1 - \varphi_2|$ by passing to the conformal map φ of the component Ω of $\Omega_1 \cap \Omega_2$ containing 0 (which now is included in Ω_j) does not seem to work, as the geometry of Ω cannot be controlled. Nevertheless, for the case of disc-chain domains, the above estimate can be proved, even without any further assumption on the geometry on the disk-chain.

THEOREM 4.3. *Let $D_1, D_2, \dots, D_n$ be a closed ε-disc-chain surrounding 0. Suppose $\partial\Omega_j \subset \bigcup_k \overline{D_k}$ for $j = 1, 2$, and let $\varphi_j : \Omega_j \to \mathbb{D}$ be conformal maps with $\varphi_1(0) = \varphi_2(0) = 0$ and $\varphi_1(p) = \varphi_2(p)$ for a point $p \in \partial\Omega_1 \cap \partial\Omega_2$. Then*

$$\sup_{w \in \Omega_1 \cap \Omega_2} |\varphi_1(w) - \varphi_2(w)| \le C\epsilon^{1/2} \log \frac{1}{\epsilon},$$

where C depends on $\operatorname{dist}(0, \bigcup_k D_k)$ only.

In case we have control on the geometry of the domains, we have the following counterpart to Corollary 4.2.

THEOREM 4.4. *If Ω_1 and Ω_2 are K-quasidiscs, if $d_H(\partial\Omega_1, \partial\Omega_2) \le \epsilon$, and if $\varphi_1(p_1) = \varphi_2(p_2)$ for a pair of points $p_j \in \partial\Omega_j$ with $|p_1 - p_2| \le \epsilon$, then*

$$\sup_{w \in \Omega} |\varphi_1(w) - \varphi_2(w)| \le C\epsilon^\alpha$$

with $\alpha = \alpha(K) \to 1$ as $K \to 1$, where Ω is the component of $\Omega_1 \cap \Omega_2$ containing 0.

The proofs of both theorems rely on the following harmonic measure estimate, which is an immediate consequence of a theorem of Marchenko [M] (see [W, section 3] for the statement and a proof). To keep this paper self-contained, we include a simple proof, shown to us by John Garnett, for which we thank him.

LEMMA 4.5. *Let $0 < \theta < \pi$, $0 < \epsilon < 1/2$, and set $D = \mathbb{D} \setminus \{re^{it} : -\theta \le t \le \theta, 1 - \epsilon \le r < 1\}$, $A = \partial D \setminus \partial\mathbb{D}$. Then*

$$\omega(0, A, D) \le \frac{\theta}{\pi} + C\epsilon \log \frac{1}{\epsilon}$$

for some universal constant C.

Proof. Set $\omega(z) = \omega(z, A, D)$ for $z \in D$. By the mean value property, it is enough to show that

$$\omega(z) \le C\frac{\epsilon}{t - \theta}$$

for $z = (1 - \epsilon)e^{it}$ and $\theta + \epsilon \le t \le \pi$. To this end, set $I = \{e^{i\tau} : -\theta \le \tau \le \theta\}$ and consider the circular arc $\{\zeta : \omega(\zeta, I, \mathbb{D}) = \frac{1}{3}\}$. If $\epsilon < \epsilon_0$ for some universal ϵ_0 (for $\epsilon \ge \epsilon_0$ there is nothing to prove), then A is disjoint from this arc and it follows that

$\omega(\zeta, I, \mathbb{D}) \geq \frac{1}{3}$ on A. The maximum principle implies $\omega(\zeta) \leq 3\omega(\zeta, I, \mathbb{D})$ on D. Now the desired inequality follows from

$$\omega((1-\epsilon)e^{it}, I, \mathbb{D}) = \frac{1}{2\pi} \int_{-\theta}^{\theta} \frac{1-(1-\epsilon)^2}{|(1-\epsilon)e^{it} - e^{i\tau}|^2} d\tau \leq C\epsilon \int_{-\theta}^{\theta} \frac{1}{(t-\tau)^2} d\tau < C\frac{\epsilon}{t-\theta}. \qquad \square$$

Proof of Theorem 4.3. We may assume that $\varphi_j(p) = 1$. We will first assume that p is one of the points $D_k \cap D_{k+1}$. Denote by Ω the largest simply connected domain $\subset \mathbb{C}$ containing 0 whose boundary is contained in $\bigcup_k D_k$ (thus $\overline{\Omega}$ is the union of $\bigcup_k D_k$ and the bounded component of $\mathbb{C} \setminus \bigcup_k D_k$), and φ is the conformal map from Ω to $\mathbb{D}$ with $\varphi(0) = 0$ and $\varphi(p) = 1$. First, let $z \in \partial\Omega_1 \cap \partial\Omega$. Denote by B, respectively, B_1, the arc of $\partial\Omega$ $(\partial\Omega_1)$ from p to z. By the Beurling projection theorem (or the distortion theorem), every $\varphi(D_j)$ has diameter $\leq C\sqrt{\epsilon}$. Therefore, $\varphi(B_1)$ is an arc in $\overline{\mathbb{D}}$, with the same endpoints as $\varphi(B)$, that is contained in $S = \{re^{it} : 1 - C\sqrt{\epsilon} \leq r < 1, -C\sqrt{\epsilon} < t < \arg\varphi(z) + C\sqrt{\epsilon}\}$. Denote $A = \partial S$. By Lemma 4.5,

$$\omega(0, B_1, \Omega_1) \leq \omega(0, B_1, \Omega \setminus B_1) \leq \omega(0, A, \mathbb{D} \setminus A) \leq \frac{1}{2\pi} \arg\varphi(z) + 2C\sqrt{\epsilon} + C\sqrt{\epsilon}\log\frac{1}{\sqrt{\epsilon}}$$

and we obtain

$$\arg\varphi_1(z) = 2\pi\omega(0, B_1, \Omega_1) \leq \arg\varphi(z) + C\epsilon^{1/2}\log\frac{1}{\epsilon}.$$

The same argument, applied to the other arc from p to z, gives the opposite inequality, and together it follows that

$$|\varphi(z) - \varphi_1(z)| \leq C\epsilon^{1/2}\log\frac{1}{\epsilon}.$$

Now let $z \in \partial\Omega_1$ be arbitrary. If z' is a point of $\partial\Omega_1 \cap \partial\Omega$ in the same disc D_j as z, then we have

$$|\varphi(z) - \varphi_1(z)| \leq |\varphi(z) - \varphi(z')| + |\varphi(z') - \varphi_1(z')| + |\varphi_1(z) - \varphi_1(z')| \leq 2C\sqrt{\epsilon} + C\epsilon^{1/2}\log\frac{1}{\epsilon}.$$

The maximum principle yields $|\varphi - \varphi_1| \leq C\epsilon^{1/2}\log\frac{1}{\epsilon}$ on Ω_1. The same argument applies to $|\varphi - \varphi_2|$, and the theorem follows from the triangle inequality.

If $p \in \partial\Omega_1 \cap \partial\Omega_2$ is arbitrary, let p' be one of the points $D_k \cap D_{k+1}$ in the same disc D_j as p. Then the above estimate, applied to a rotation of φ_1, φ_2, and p', gives $|\varphi_2(p')/\varphi_1(p')\varphi_1 - \varphi_2| \leq C\epsilon^{1/2}\log\frac{2}{\epsilon}$, and the theorem follows from $|\varphi_j(p) - \varphi_j(p')| \leq C\sqrt{\epsilon}$. $\square$

The following lemma is another easy consequence of the aforementioned theorem of Marchenko [M] (see [W, section 3]).

LEMMA 4.6. *Let $H \subset \mathbb{D}$ be a K-quasidisc with $0 \in H$ such that $\partial H \subset \{1 - \epsilon < |z| < 1\}$, and let h be a conformal map from $\mathbb{D}$ to H with $h(0) = 0$ and $|h(p) - p| < \epsilon$ for some $p \in \partial\mathbb{D}$. Then*

$$|h(z) - z| \leq C\epsilon\log\frac{1}{\epsilon},$$

where C depends on K only.

Proof. We may assume that $p = 1$. Let $z = e^{i\tau}$ and consider the arc $A = \{h(e^{it}) : 0 \leq t \leq \tau\} \subset \partial H$ of harmonic measure $\tau/2\pi$. For a suitable constant C, depending

on K, we have that $D = \mathbb{D} \setminus \{re^{it} : -C\epsilon \leq t \leq \arg h(z) + C\epsilon, 1 - \epsilon \leq r < 1\}$ contains A. By the maximum principle and Lemma 4.5,

$$\tau/2\pi = \omega(0, A, H) \leq \omega(0, \partial D \cap \mathbb{D}, D) \leq \arg h(z)/2\pi + C\epsilon \log \frac{1}{\epsilon}.$$

Applying the same reasoning to $\partial H \setminus A$, the lemma follows for all $z \in \partial \mathbb{D}$ and thus for all $z \in \mathbb{D}$.   □

Note that the conclusion of Lemma 4.6 is true if, instead of assuming that H is a K-quasidisc, we assume only that $\arg z$ is increasing on ∂H.

Proof of Theorem 4.4. Because Ω_1 and Ω_2 are K-quasidiscs, φ_1 and φ_2 have K^2-quasiconformal extensions to $\mathbb{C}$ (see [L, Chapter I.6]). In particular, they are Hölder continuous with exponent $1/K^2$ (see [A]), and it follows that with $\alpha = 1/K^2$ and $r = 1 - C\epsilon^\alpha$, we have $\varphi_1^{-1}(\{|z| \leq r\}) \subset \Omega_2$. In particular, $h(z) = \varphi_2(\varphi_1^{-1}(rz))$ is a conformal map from $\mathbb{D}$ onto a K^4-quasidisc $H \subset \mathbb{D}$, and by the Hölder continuity of φ_2 and φ_1^{-1} we have $\partial H \subset \{1 - C\epsilon^{\alpha^3} < |z| < 1\}$. Now Lemma 4.6 yields $|h(z) - z| \leq C\epsilon^\beta$ for any $\beta < \alpha^3$ and $C = C(\beta)$. For $w \in \Omega \subset \Omega_1 \cap \Omega_2$, let $z = \varphi_1(w)$; then

$$|\varphi_1(w) - \varphi_2(w)| = |z - \varphi_2(\varphi_1^{-1}(z))|$$
$$\leq |z - \varphi_2(\varphi_1^{-1}(rz))| + |\varphi_2(\varphi_1^{-1}(rz)) - \varphi_2(\varphi_1^{-1}(z))| \leq C\epsilon^\beta,$$

where again we have used the Hölder continuity of φ_2 and φ_1^{-1}. The theorem follows.   □

5. Convergence of the mapping functions. We will now combine the results of sections 2 and 3 with the estimates of the previous section to obtain quantitative estimates on the convergence of the geodesic algorithm. Throughout this section, Ω will denote a given simply connected domain containing 0, bounded by a Jordan curve $\partial \Omega$, $z_0, \ldots, z_n$ are consecutive points on $\partial \Omega$, Ω_c is the domain and $\varphi_c : \Omega_c \to \mathbb{D}$ is the map computed by the geodesic algorithm, and $\varphi : \Omega \to \mathbb{D}$ is a conformal map, normalized so that $\varphi_c(0) = \varphi(0) = 0$ and $\varphi_c(p_0) = \varphi(p_0)$ for some $p_0 \in \partial \Omega \cap \partial \Omega_c$.

Combining Theorems 2.2 and 4.3 and Propositions 2.5 and 3.12 we immediately obtain the following theorem.

THEOREM 5.1. *If $\partial \Omega$ is contained in a closed ϵ-disc-chain $\bigcup_{j=0}^n \overline{D_j}$ and if $z_j = \partial D_j \cap \partial D_{j+1}$, then $\partial \Omega_c$ is a smooth $(C^{\frac{3}{2}})$ piecewise analytic Jordan curve contained in $\bigcup_{j=0}^n D_j \cup z_j$, the map φ_c extends to be conformal on $\Omega \cup \Omega_c$, and*

$$\sup_{w \in \Omega} |\varphi(w) - \varphi_c(w)| \leq C\epsilon^{1/2} \log \frac{1}{\epsilon}.$$

Now assume that $\partial \Omega$ is a K-quasicircle with $K < K_0$, and assume approximate equal spacing of the z_j, say, $\frac{1}{2}\epsilon < |z_{j+1} - z_j| < 2\epsilon$. Then

$$(5.1) \qquad\qquad \frac{C}{\epsilon} \leq n \leq \frac{C}{\epsilon^d},$$

where d (essentially the Minkowski dimension) is close to 1 when K is close to 1. Combining Theorem 3.11 with Corollary 4.2 and Theorem 4.4, we have the following theorem.

THEOREM 5.2. *Suppose $\partial \Omega$ is a K-quasicircle with $K < K_0$. The Hausdorff distance between $\partial \Omega$ and $\partial \Omega_c$ is bounded by $C'(K)\epsilon$, where $C'(K)$ is a constant depending upon K that tends to 0 as K tends to 1 and n to infinity. Furthermore,*

$$||\varphi^{-1} - \varphi_c^{-1}||_\infty \leq C\epsilon^\alpha$$

and

$$\sup_{w\in\Omega_0} |\varphi(w) - \varphi_c(w)| \le C\epsilon^\alpha$$

with $\alpha = \alpha(K) \to 1$ as $K \to 1$, where Ω_0 is the component of $\Omega \cap \Omega_c$ containing 0.

The best possible exponent in (5.1) in terms of the standard definition of $K(\partial\Omega)$, which slightly differs from our geometric definition, is given by Smirnov's (unpublished) proof of Astala's conjecture,

$$d \le 1 + \left(\frac{K-1}{K+1}\right)^2.$$

This allows us to easily convert estimates given in terms of ε, as in Theorem 5.2, into estimates involving n.

Finally, assume that $\partial\Omega$ is a smooth closed Jordan curve. Then Ω is a K-quasicircle and a John-domain by the uniform continuity of the derivative of the arc length parameterization of $\partial\Omega$. The quasiconformal norm $K(\partial\Omega)$ and the John constant depend on the global geometry, as does the ε-pacman condition when there are not very many data points. As the example in Figure 11 shows, even an infinitely differentiable boundary can have a large quasiconformal constant and a large John constant. However, the ε-pacman condition becomes a local condition if the mesh size $\mu(\{z_k\}) = \max_k |z_{k+1} - z_k|$ of the data points is sufficiently small. The radii of the balls in the definition of the ε-pacman condition

(5.2)
$$R_k = C_1 \frac{|z_{k+1} - z_k|}{\varepsilon^2}$$

increase as ε decreases but can be chosen small for a fixed ε if the mesh size μ is small. To apply the geodesic algorithm we suppose that the data points have small mesh size and, as in the proof of Theorem 3.10, $|(z_0 - z_n)/(z_{n-1} - z_n)|$ is sufficiently large so that the ε-diamond-chain $D(z_0, z_1), \ldots, D(z_{n-1}, z_n)$ satisfies the ε-pacman condition and

$$\partial\Omega \subset \bigcup_{k=0}^n D(z_k, z_{k+1}),$$

where $D(z_n, z_{n+1}) = D(z_n, z_0)$ is an ε-diamond. This can be accomplished for smooth curves by taking data points $z_0, \ldots, z_n, z_0$ with small mesh size and discarding the last few $z_{n-n_1}, \ldots, z_n$, where n_1 is an integer depending on ε and on $\partial\Omega$. The remaining subset still has small mesh size (albeit larger). This process of removing the last few data points is necessary to apply the proof of Theorem 3.10, but in practice it is omitted. We view it only as a defect in the method of proof.

If $\partial\Omega \in C^1$ and if φ is a conformal map of Ω onto $\mathbb{D}$, then $\arg(\varphi^{-1})'$ is continuous. Indeed, it gives the direction of the unit tangent vector. However, there are examples of C^1 boundaries where φ' and $(\varphi^{-1})'$ are not continuous. In fact, it is possible for both to be unbounded. If we make the slightly stronger assumption that $\partial\Omega \in C^{1+\alpha}$ for some $0 < \alpha < 1$, then $\varphi \in C^{1+\alpha}$ and $\varphi^{-1} \in C^{1+\alpha}$ by Kellogg's theorem (see [GM, p. 62]). In particular, the derivatives are bounded above and below on $\overline{\Omega}$ and $\overline{\mathbb{D}}$, respectively. Because of Proposition 3.12, we will consider the case $1 + \alpha = 3/2$. Similar results are true for $1 + \alpha < 3/2$.

THEOREM 5.3. *Suppose $\partial\Omega$ is a closed Jordan curve in $C^{3/2}$ and φ is a conformal map of Ω onto $\mathbb{D}$. Suppose $z_0, z_1, \ldots, z_n, z_0$ are data points on $\partial\Omega$ with mesh size $\mu = \max|z_j - z_{j+1}|$. Then there is a constant C_1 depending on the geometry of $\partial\Omega$, so that the Hausdorff distance between $\partial\Omega$ and $\partial\Omega_c$ satisfies*

$$(5.3) \qquad\qquad d_H(\partial\Omega, \partial\Omega_c) \le C_1\mu^{3/2}$$

and the conformal map φ_c satisfies

$$(5.4) \qquad\qquad ||\varphi^{-1} - \varphi_c^{-1}||_\infty \le C\mu^p$$

and

$$(5.5) \qquad\qquad \sup_{z\in\Omega\cap\Omega_c} |\varphi(z) - \varphi_c(z)| \le C\mu^p$$

for every $p < 3/2$.

For example, if n data points are approximately evenly spaced on $\partial\Omega$, so that $\mu = C/n$, then the error estimates are of the form $C/n^{3/2}$ in (5.3) and C/n^p for $p < 3/2$ in (5.4) and (5.5). While Theorem 5.3 gives simple estimates in terms of the mesh size or the number of data points, smaller error estimates can be obtained with fewer data points if the data points are distributed so that there are fewer on subarcs where $\partial\Omega$ is flat and more where the boundary bends or where it folds back on itself. In other words, construct diamond-chains with angles ε_k satisfying the ε_k-pacman condition centered at z_k for each k. The errors will then be given by

$$\max_k\big(\varepsilon_k|z_k - z_{k+1}|\big)^p.$$

Proof. It is not hard to see from (5.2) that $\partial\Omega$ satisfies the ϵ-pacman condition with

$$\epsilon = C\mu^{1/2}$$

for C sufficiently large. By the proof of Theorem 3.10, $\partial\Omega_c$ is contained in the union of the diamonds. The diamonds $D(z_k, z_{k+1})$ have angle $C\mu^{1/2}$ and width bounded by $C\mu$, and therefore (5.3) holds.

Let ψ be a conformal map of $\mathbb{D}$ onto the complement of $\overline{\Omega}$, $\mathbb{C}^* \setminus \overline{\Omega}$. Then by Kellogg's theorem, as mentioned above, $\psi \in C^{3/2}$. In particular, $|\psi'|$ is bounded above and below on $1/2 < |z| < 1$. By the Koebe distortion theorem there are constants C_1, C_2 so that

$$C_1(1 - |z|) \le \text{dist}(\psi(z), \partial\Omega) \le C_2(1 - |z|)$$

for all z with $1/2 < |z| < 1$. Thus we can choose $r = 1 - C_3\mu^{3/2}$ so that the image of the circle of radius r, $I_r = \psi(\{|z| = r\})$, does not intersect the diamond-chain and $d_H(I_r, \partial\Omega) \sim \mu^{3/2}$. Then the bounded component of the complement of I_r is a Jordan region U_r containing Ω and bounded by $I_r \in C^{3/2}$, with $C^{3/2}$ norm dependent only on $\partial\Omega$, and the bounds on $|\psi'|$.

Let σ be a conformal map of U_r onto $\mathbb{D}$. Inequality (5.4) now follows from [W, Theorem VIII] by comparing the conformal maps φ^{-1} and φ_c^{-1} to the conformal map σ^{-1}, where $\sigma : U_r \to \mathbb{D}$ and where all three (inverse) conformal maps are normalized to have positive derivative at 0 and map 0 to the same point in Ω.

To see (5.5), note that

$$\sigma(\partial\Omega \cup \partial\Omega_c) \subset \{z : 1 - |z| < c\mu^{3/2}\}.$$

Moreover, because $\partial\Omega \cup \partial\Omega_c$ is contained in the diamond-chain, and because both $\sigma \in C^{3/2}$ and $\sigma^{-1} \in C^{3/2}$, $\arg\sigma(\zeta)$ is increasing along $\partial\Omega$ for μ sufficiently small. By the remark after the proof of Lemma 4.6,

$$|\omega(0, \gamma, \sigma(\Omega)) - \omega(0, \gamma^*, \mathbb{D})| \leq C\mu^{3/2}\log\mu$$

for every subarc γ of $\sigma(\partial\Omega)$, where γ^* denotes the radial projection of γ onto $\partial\mathbb{D}$. The same statements are true for $\partial\Omega_c$. Then (5.5) follows because the harmonic measure of the subarc γ_p of $\partial\Omega$ from p_0 to p is given by

$$\omega(0, \gamma_p, \Omega) = \frac{1}{2\pi}\arg\left(\frac{\varphi(p)}{\varphi(p_0)}\right),$$

and a similar statement is true for φ_c.   □

The constant C in Theorem 5.3 depends on the quasiconformality constant $K = K(\partial\Omega)$, p, $\mathrm{diam}(\Omega)$, $\mathrm{dist}(0, \partial\Omega)$, and

$$M = \sup_{1/2 < |z| < 1}\left(|\psi'|, 1/|\psi'|\right),$$

where ψ is a conformal map of the complement of Ω to $\mathbb{D}$. If $I_r = \psi(\{|z| = r\})$ is replaced by a $C^{3/2}$ curve which is constructed geometrically instead of using the conformal map ψ, then the constant C can be taken to depend only on the geometry of the region Ω.

Similar results, albeit more complicated, for uniform convergence of the derivatives of the computed maps and the derivatives of their inverses could also be obtained from the results in [W2, Theorems III and V].

6. Some numerical results. An in-depth comparision of the algorithms in this article with other methods of conformal mapping and convergence rates will be written separately. To give the reader a sense of the speed and accuracy of computations, if 10,000 data points are given, it takes about 25 seconds with the geodesic algorithm to compute the conformal maps to the interior, the exterior, and their inverses on a 3.2 GHz Pentium IV computer. Since all of the basic maps are given explicitly in terms of elementary maps, the speed depends only on the number of points and not the shape of the region or the distribution of the data points. The accuracy can be measured if the true conformal map is known. For example,

$$f(z) = \frac{rz}{1 - (rz)^2},$$

where $r < 1$ maps the unit disc into an inverted ellipse. See Figure 12.

The region was chosen because it almost pinches off at 0, and because the stretching/compression given by $\max|f'|/\min|f'|$ is big for r near 1. This is sometimes called the "crowding phenomenon." We chose $r = .95$ and used as data points the image by f of 10,000 equally spaced points on the unit circle, and we compared the corresponding points on the unit circle computed by the geodesic algorithm with 10,000 equally spaced points. The errors were less than $1.8 \cdot 10^{-6}$. The same procedure using the zipper algorithm took 84 seconds and had errors less than $9.2 \cdot 10^{-8}$. When
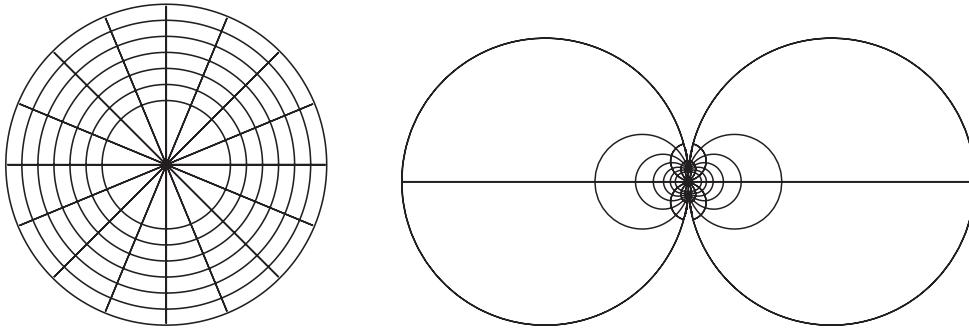
FIG. 12. *Inverted ellipse with $r = .95$.*

the number of data points was increased to 100,000, the time to run the geodesic algorithm increased to 25 minutes with errors less than $2 \cdot 10^{-8}$. In this example, the difference between successive (given) boundary data points on the inverted ellipse ranged from $.025$ to $3 \cdot 10^{-6}$ so that perhaps a better distribution of data points would have given even smaller errors.

In practice, the choice of data points corresponding to equally spaced points on the circle is not available. An alternative approach to this example is to select data points on the inverted ellipse which are approximately equally spaced in arc length. However, if we choose 10,000 points in this manner, then three consecutive points at the inward pointing "tips" of the region form a "turning angle" of more than $100°$ because the curvature is so large. This leads to relatively large errors in the map since the tip has large harmonic measure. Another method is to select data points so that the "turning angle"

$$\left| \arg\left(\frac{z_{k+1} - z_k}{z_k - z_{k-1}} \right) \right|$$

is not too big. This results in inaccuracies for this region because the curvature rapidly decreases to zero near the tips, and hence the data points are not very "evenly spaced."

A better method is to use a combination of these ideas. We generated a list of 10^6 points on the boundary of the inverted ellipse and then selected a subset using the following criteria: Having selected $z_1, \ldots, z_k$, choose z_{k+1} to be the first data point in the list after z_k satisfying

$$\left| \arg\left(\frac{z_{k+1} - z_k}{z_k - z_{k-1}} \right) \right| > \delta$$

or

$$\log \left| \frac{z_{k+1} - z_k}{z_k - z_{k-1}} \right| > \delta.$$

To compare with our previous results, we selected $\delta = .0025$ and thereby obtained 9,890 data points with the property that the "turning angle" is small and the ratio of lengths of successive arcs is close to 1. We compared the points on the unit circle obtained from the geodesic algorithm with the true inverse images. The maximal error was less than 5.3×10^{-6}. It is interesting to note that the maximal distance between successive points on the unit circle is 4.2×10^{-2} so that the errors are much
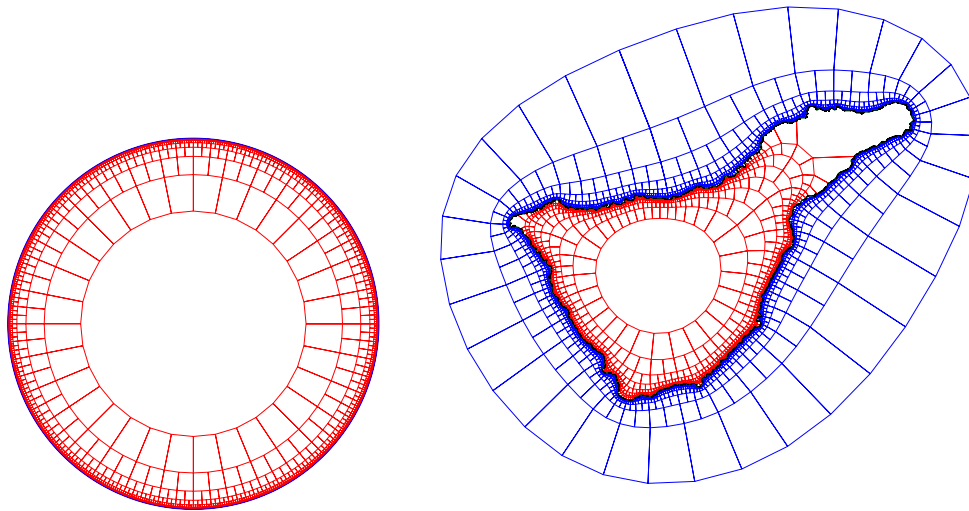
FIG. 13. *Tenerife.*

smaller than the harmonic measure of the corresponding arcs. This technique can be applied to any region where the boundary is known at a very large number of points.

Figure 13 shows the conformal map of a Carleson grid on the disc to both the interior and exterior of the island Tenerife (Canary Islands). We chose this region to illustrate the method on a nonsmooth region where no symmetry is involved. The center of the interior is the volcano Teide. It also shows both the original data for the coastline, connected with straight line segments, and the boundary curve connecting the data points using the zipper algorithm. At this resolution, it is not possible to see the difference between these curves. The zipper algorithm was applied to 6,168 data points and took 36 seconds. The image of 24,673 points on the unit circle took 48 seconds, and all of these points were within $9 \cdot 10^{-5}$ of the polygon formed by connecting the 6,168 data points. The points on the circle corresponding to the 6,168 vertices were mapped to points within 10^{-10} of the vertices. This error is due to the tolerance set for Newton's method, round-off error, and the compression/expansion of harmonic measure. The image of 8,160 vertices in the Carleson grid took 25 seconds to be mapped to the interior and 25 seconds to the exterior.

The first objection one might have in applying these algorithms with a large number of data points is that compositions of even very simple analytic maps can be quite chaotic. Indeed, this is the subject of the field of complex dynamics. We could redefine the basic maps f_a by composing with a linear fractional transformation of the upper-half plane so that the composed map is asymptotic to z as $z \to \infty$. This will not affect the computed curve in these algorithms since the next basic map begins with a linear fractional transformation (albeit altered). However, if we formulate the basic maps in this way, then because the maps are nearly linear near ∞, the numerical errors will accumulate only linearly.

Banjai and Trefethen [BT] adapted fast multipole techniques to the Schwarz–Christoffel algorithm and successfully computed the conformal map to a region which is bounded by a polygon with about 10^5 edges. They used a 12-fold symmetry in the region to immediately reduce the parameter problem to size 10^4. Any other

conformal mapping technique can also use symmetry and obtain a 12-fold reduction in the number of data points required; however, their work does show at least that Schwarz–Christoffel is possible with 10^4 vertices, though convergence of the algorithm to solve the parameter problem is not always ensured. The time it takes to run the zipper algorithm and the resulting accuracy for these snowflake regions is very close to the timing and accuracy for the fast multipole improvements in the Schwarz–Christoffel method. The geodesic algorithm is almost as good and has the advantage that it is very easy to code and convergence can be proved. For a region bounded by a polygon with a small number of vertices, where high accuracy is desired (for instance, errors on the order of 10^{-14}), the Schwarz–Christoffel method is preferable. It would be interesting to try to prove convergence of the technique used in [BT] to find the prevertices in the Schwarz–Christoffel representation for polygons which are K-quasicircles in terms of K. It would be interesting as well to apply multipole techniques to the zipper algorithm. A first step in this direction can be found in Kennedy [KT].

One additional observation worth repeating in this context is that the geodesic and zipper algorithms *always* compute a conformal map of $\mathbb{H}$ to a region bounded by a Jordan curve passing through the data points, even if the disc-chain or pacman conditions are not met. The image region can be found by evaluating the function at a large number of points on the real line. By Proposition 2.5 and Corollary 3.9, if the data points $\{z_j\}$ satisfy the hypotheses of Theorem 2.2 or 3.4, then φ can be analytically extended to be a conformal map of the original region Ω to a region very close to $\mathbb{D}$. To do so requires careful consideration of the appropriate branch of $\sqrt{z}$ at each stage of the composition.

Theorems 2.2 and 3.4 and their proofs suggest how to select points on the boundary of a region to give good accuracy for the mapping functions. Roughly speaking, points need to be chosen closer together where the region comes close to folding back on itself. See Figure 12, for example. Greater accuracy can be obtained by placing more points on the boundary near the center and fewer on the big lobes. See also the remarks after Theorem 5.3 in this regard. In practice, the zipper map works well if points are distributed so that

$$(6.1) \qquad\qquad B(z_k, 5|z_{k+1} - z_k|) \cap \partial\Omega$$

is connected.

When the boundary of the given region is not smooth, then one of the processes described in section 2 should be used to generate the boundary data, if the geodesic algorithm is to be used. For example, if nothing is known about the boundary except for a list of data points, then we preprocess the data by taking data points along the line segments between the original data points, so that these new points correspond to points of tangency of disjoint circles centered on the line segments, including circles centered at the original data points. Note that the original boundary points are not among these new data points. The geodesic algorithm then finds a conformal map to a region with the new data points on the boundary. The boundary of the new region will be close to the polygonal curve through the original data points but will not pass through the original data points. This boundary is "rounded" near the original data points. Indeed, it is a smooth curve.

When the boundary of the desired region is less smooth, for example, with "corners," then the zipper or slit algorithms should be used. In this case additional points are placed along the line segments between the data points, with at least five points

per edge and satisfying (6.1). In practice, at least 500 points are chosen on the boundary so that the image of the circle will be close to the polygonal line through the data points. Since two data points are pulled down to the real line with each basic map in the zipper algorithm, the original data points should occur at even numbered indices in the resulting data set (the first data point is called z_0). Then the computed boundary Ω_c will have corners at each of the original data points, with angles very close to the angles of the polygon through the original data points.

Fortran programs for a version of the zipper algorithm can be obtained from [MD]. Also included is a graphics program, written in C with X-11 graphics by Mike Stark, for the display of the conformal maps. There are also several demo programs applying the algorithm to problems in elementary fluid flow, extremal length, and hyperbolic geometry. Extensive testing of the geodesic algorithm [MM] and an early version of the zipper algorithm was done in the 1980s with Morrow. In particular, that experimentation suggested the initial function φ_0 in the zipper algorithm which maps the complement of a circular arc through z_0, z_1, and z_2 onto $\mathbb{H}$.

Appendix. Jørgensen's theorem. Since Jørgensen's theorem is a key component of the proof of the convergence of the geodesic algorithm, we include a short self-contained proof. It says that discs are strictly convex in the hyperbolic geometry of a simply connected domain Ω (unless $\partial\Omega$ is contained in the boundary of the disk).

THEOREM A.1 (Jørgensen [J]). *Suppose Ω is a simply connected domain. If Δ is an open disc contained in Ω and if γ is a hyperbolic geodesic in Ω, then $\gamma \cap \Delta$ is connected, and if it is nonempty, it is not tangent to $\partial\Delta$ in Ω.*

Proof (see [P, pp. 91–93]). Applying a linear fractional transformation to Ω, we replace the disc Δ by the upper-half plane $\mathbb{H}$. Suppose $x \in \mathbb{R}$ and suppose that f is a conformal map of $\mathbb{D}$ onto Ω such that $f(0) = x$ and $f'(0) > 0$. We will use the auxiliary function $z + 1/z$, which is real-valued on $\partial\mathbb{D} \cup (-1,1)$. Then

$$\text{Im}\left(\frac{f'(0)}{f(z)-x} - \left(\frac{1}{z}+z\right)\right)$$

is a bounded harmonic function on $\mathbb{D}$ which is greater than or equal to 0 by the maximum principle. Thus $\text{Im}\frac{f'(0)}{f(z)-x} \geq 0$ on $(-1,1)$, and hence $\text{Im} f(z) \leq 0$ on the diameter $(-1,1)$. The condition $f'(0) > 0$ means that the geodesic $f\big((-1,1)\big)$ is tangent to $\mathbb{R}$ at x. Two circles which are orthogonal to $\partial\mathbb{D}$ can meet in $\mathbb{D}$ in at most one point, and hence hyperbolic geodesics in simply connected domains (images of orthogonal circles) meet in at most one point and are not tangent. Thus if γ is a geodesic in Ω which intersects $\mathbb{H}$ and contains the point x, then it cannot be tangent to $\mathbb{R}$ at x and cannot re-enter $\mathbb{H}$ after leaving it at x because it is separated from $\mathbb{H}$ by the geodesic $f\big((-1,1)\big)$. The theorem follows. ☐

In section 2, we commented that a constructive proof of the Riemann mapping theorem followed from the proof of Theorem 2.2. The application of Jørgensen's theorem in the proof of Theorem 2.2 is only to domains for which the Riemann map has been explicitly constructed.

REFERENCES

[A]   L. Ahlfors, *Lectures on Quasiconformal Mappings*, Van Nostrand, Princeton, NJ, 1966.

[BT]   L. Banjai and L. N. Trefethen, *A multipole method for Schwarz–Christoffel mapping of polygons with thousands of sides*, SIAM J. Sci. Comput., 25 (2003), pp. 1042–1065.

[GM]   J. Garnett and D. E. Marshall, *Harmonic Measure*, Cambridge University Press, New York, 2005.

[H]   P. Henrici, *Applied and Computational Complex Analysis, Vol.* 3, John Wiley & Sons, New York, 1986.

[J]   V. Jørgensen, *On an inequality for the hyperbolic measure and its applications in the theory of functions*, Math. Scand., 4 (1956), pp. 113–124.

[KT]   T. Kennedy, *Computing the Loewner Driving Process of Random Curves in the Half Plane*, preprint, http://arxiv.org/PS_cache/math/pdf/0702/0702071v1.pdf.

[K]   R. Kühnau, *Numerische Realisierung konformer Abbildungen durch "Interpolation,"* Z. Angew. Math. Mech., 63 (1983), pp. 631–637.

[L]   O. Lehto, *Univalent Functions and Teichmüller Spaces*, Springer-Verlag, New York, 1987.

[M]   A. R. Marchenko, *Sur la representation conforme*, C. R. Acad. Sci. USSR, 1 (1935), pp. 289–290.

[MD]   D. E. Marshall, *Zipper*, Fortran Programs for Numerical Computation of Conformal Maps, and C Programs for X-11 Graphics Display of the Maps. Sample pictures, Fortran, and C code available online at http://www.math.washington.edu/~marshall/personal.html.

[MM]   D. E. Marshall and J. A. Morrow, *Compositions of Slit Mappings*, manuscript, 1987.

[P]   C. Pommerenke, *Boundary Behaviour of Conformal Maps*, Springer-Verlag, Berlin, 1992.

[SK]   K. Stephenson, *Circle packing: A mathematical tale*, Notices Amer. Math. Soc., 50 (2003), pp. 1376–1388.

[T]   M. Tsuji, *Potential Theory in Modern Function Theory*, Chelsea, New York, 1975.

[W]   S. Warschawski, *On the degree of variation in conformal mapping of variable regions*, Trans. Amer. Math. Soc., 69 (1950), pp. 335–356.

[W2]   S. Warschawski, *On the distortion in conformal mapping of variable domains*, Trans. Amer. Math. Soc., 82 (1956), pp. 300–322.